

---

*Research article*

## Use of Norwegian National Test Sites to evaluate CPTU correlations embedded in software

Tom Lunne<sup>1,\*</sup>, Luisa Dhimitri<sup>2</sup>, John Powell<sup>3</sup> and Santiago Quinteros<sup>1</sup>

<sup>1</sup> Offshore Geotechnics, Norwegian Geotechnical Institute, P.O. Box 3930, Oslo N-0806, Norway

<sup>2</sup> Geotech Engineer, UK

<sup>3</sup> Geolabs Limited, Bucknalls Lane, Garston, Watford, WD25 9XX, UK

\* **Correspondence:** Email: tom.lunne@ngi.no; Tel: +47-90029267.

**Abstract:** Commercial software packages that utilise published CPTU correlations are frequently used for quick presentation of soil parameters such as soil unit weight, over consolidation ratio, undrained shear strength, lateral stress ratio, and peak friction angle. It is a well-known fact that such correlations are not globally valid, but many practitioners use the parameters obtained this way even in foundation design. At the Norwegian soft clay, quick clay, silt, and sand sites, high quality sampling and laboratory testing have resulted in a consistent representative database of reliable soil parameters. Moreover, high quality results of CPTU, seismic cones, self-boring pressuremeter and a novel flow cone tool are also available at the sites. Using these high-quality benchmark parameters gives an excellent opportunity to evaluate the validity of the soil parameters derived from 18 published CPTU correlations used in commercial software packages. For transparency, the correlations are described in some detail with full reference to the source. A comparison of correlation derived parameters and reliable laboratory-based benchmark soil parameters showed that the use of global correlations can be too conservative and, in some cases, dangerous. Local correlations are not only recommended but are essential for design. In this study, we did not cover highly overconsolidated clays and very dense sands, though similar conclusions on those soils may be expected.

**Keywords:** CPT correlations; clay; quick clay; silt; sand; high-quality samples; unit weight

---

## 1. Introduction

Commercial software packages that utilise published CPTU correlations are frequently used for quick evaluation of soil parameters such as soil unit weight, overconsolidation ratio, undrained shear strength, lateral stress ratio, peak friction angle, and shear wave velocity. It is a well-known fact that such correlations are not globally valid, but many practitioners use the parameters obtained this way in foundation design.

In the period 2016–2019, the Norwegian Geo Test Site (NGTS) project [1] was established. Figure 1.1 shows the geographical location of these five Norwegian test sites. Two of the sites are in southeastern Norway; the soft clay site in Onsøy and the silt site in Halden. The quick clay site at Tiller-Flotten and the medium dense sand site at Øysand are both in mid-Norway, close to Trondheim. The detailed and high-quality soil characterization of these four sites is used in the study presented in this paper. In addition, there is a test permafrost site in Svalbard, which is not included in this paper.

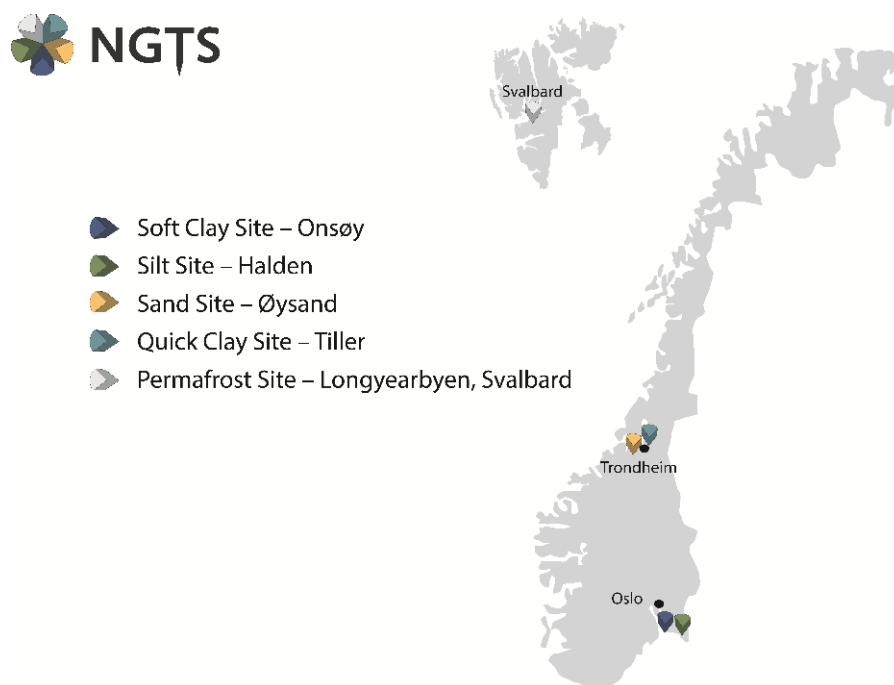


**Figure 1.1.** Location of the NGTS geotechnical research sites in Norway [2].

At these Norwegian soft-clay, silt, and sand sites, high quality sampling and laboratory testing have resulted in consistent representative and reliable soil parameters. High quality in situ data, from piezocone tests (CPTUs), seismic CPTU (SCPTUs), seismic Dilatometer Marchetti tests (SDMTs), and self-boring pressuremeters (SBPs) are also available at the sites. Using these high-quality benchmark parameters gives an excellent and novel opportunity to evaluate the validity and reliability of the soil parameters derived from published CPTU correlations used in commercial software packages.

A comprehensive and systematic comparison of correlation derived parameters and reliable laboratory-based benchmark soil parameters is presented in this paper.

## 2. Description of Norwegian National Test Sites

The four sites examined in this paper were described in detail at the ISGTS symposium in Oslo in 2019 (see [3–6]). A summary is given in the following sections.

### 2.1. Onsøy soft clay site

Because of the thickness of the clay deposit and its very uniform nature, the Onsøy site has been used for research purposes for several decades. The site is in southeastern Norway, about 100 km south of Oslo (Figure 1.1). The soils at the Onsøy site are marine clays, similar to the clays found at many sites in Norway, Sweden, and Finland. The clay was deposited during deglaciation and the early postglacial period (Holocene) at times with higher sea levels than today. Characterisation and engineering properties of the Onsøy clay have been documented in, for example, [7]. Over the years, several locations have been used for R&D purposes. The latest location is the one used for the NGTS project, which lies a couple of km south of the one described by [7].

Figure 2.1 shows classification parameters in terms of natural water content ( $w$ ), plasticity limits, and clay and silt content vs depth.

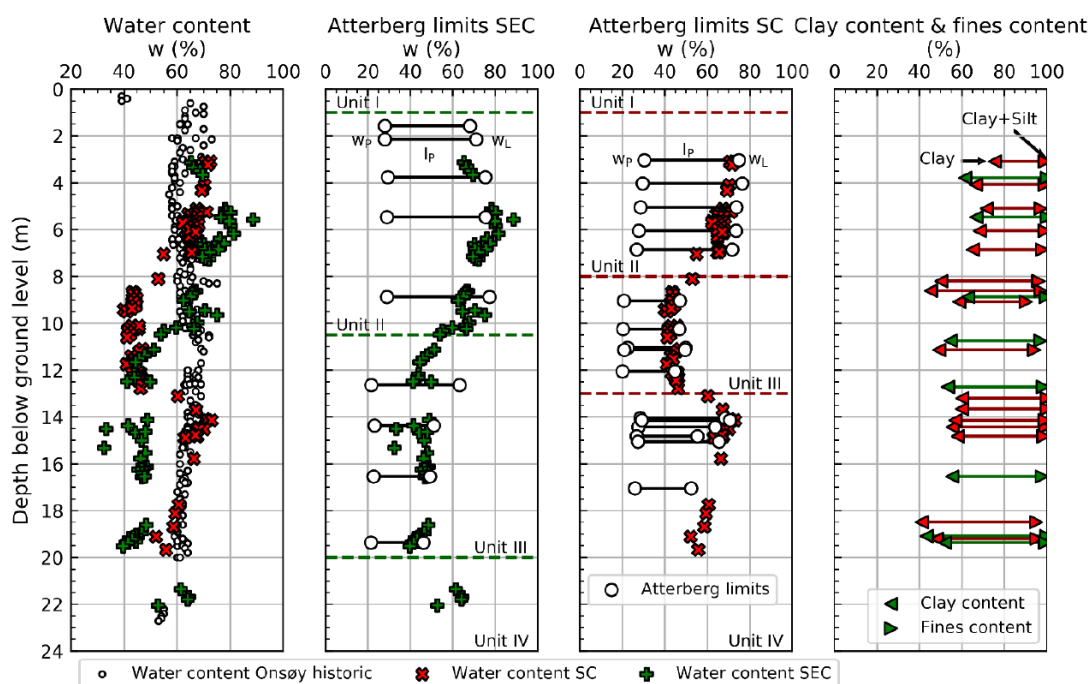


**Figure 2.1.** Water content, plasticity limits, and grain size with depth at Onsøy [3].

The overconsolidation ratio (OCR) was determined from oedometer tests on high quality Sherbrooke block samples (see [7]). The OCR at Onsøy decreases, as expected, from about 4 near the surface to 1.2 at 30 m depth. Other soil parameters are presented in the next section.

Additionally, many CPTUs have been carried out using several cone penetrometers, all adhering to [8] regarding geometry and dimension but made by different cone manufacturers. The researchers in [9] found that the corrected cone resistance,  $q_t$  (calculated as  $q_t = q_c + u_2(1 - a)$ ), and the pore pressure

measured at shoulder position,  $u_2$ , were quite consistent, while the measured  $f_s$  values varied significantly depending on the type of cone penetrometer (Figure 2.2). The  $a$  values used were determined by calibration and taken from the manufacturers' calibration certificates.

More details about the NGTS Onsøy site are found in [3].

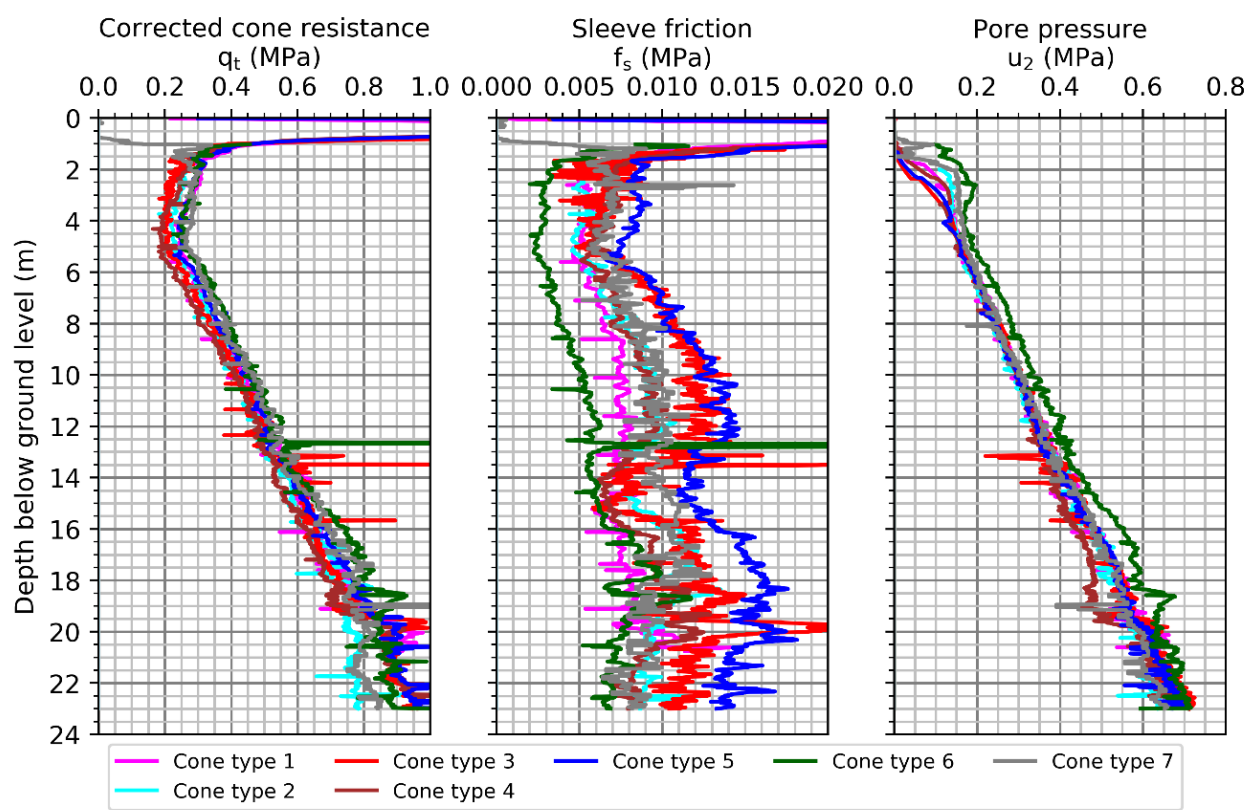


**Figure 2.2.** Corrected cone resistance,  $q_t$ , and measured  $f_s$  and  $u_2$  for the NGTS Onsøy soft clay site using seven cones (from [9]).

## 2.2. Halden silt site

The Halden site is in southeastern Norway, approximately 120 km south of Oslo (Figure 1.1). The deposit consists of marine and fjord marine sediments that emerged from the sea following a fall in relative sea level in the Oslofjord region during the last ca. 11000 years. There is up to 10 m of uniform silty soil at the site. The homogenous silt deposit at Halden has no structure. The silt layer of interest is below a 4.5 m thick layer of sand and above a 6 m thick deposit of clay. Basic parameters for the Halden silt are presented in the log in Figure 2.3. The water content in the silt decreases only slightly between depths of 4.5 to 11 m, with values at about 30%. From 11 to 15 m, the water content decreases more rapidly to about 21%. The changes in water content are reflected in the unit weight profile, with an increasing unit weight in depth. MSCLs indicate higher unit weight,  $\gamma$ , than the lab measured values. Figure 2.3 also includes the results of six CPTUs in terms of  $q_t$ ,  $u_2$ , and  $f_s$ . Similar to the Onsøy site, the results of  $q_t$  and  $u_2$  are quite consistent, while there is quite a spread in the  $f_s$  data as discussed (see also [5,10]).

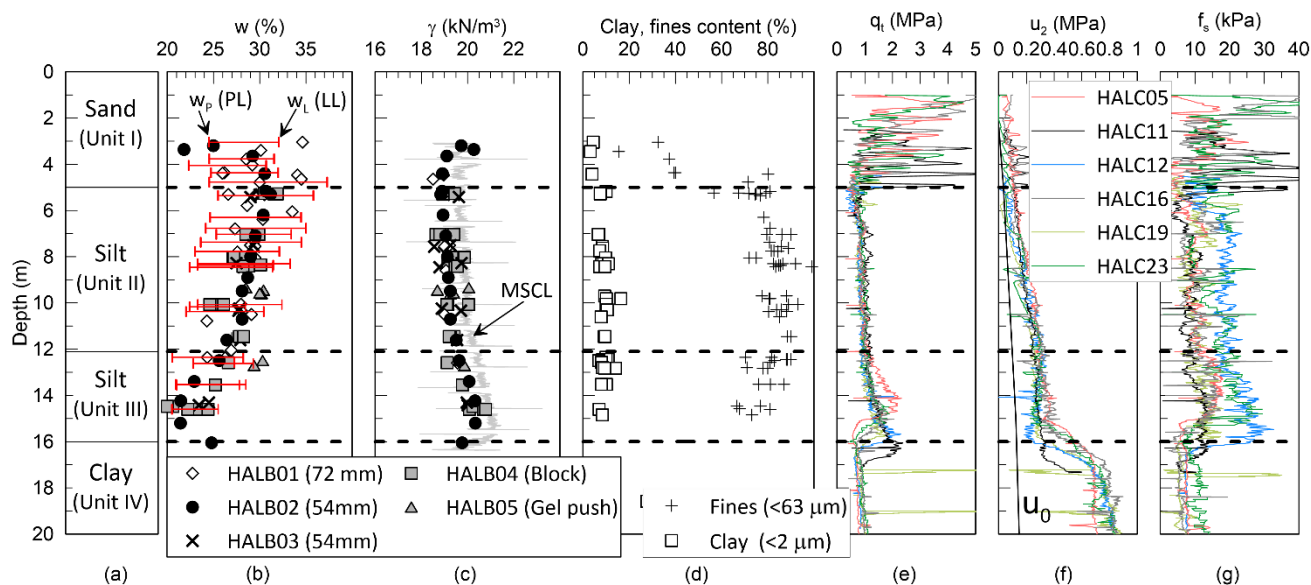


**Figure 2.3.** Classification and CPTU data; (a) soil units, (b) natural water content and Atterberg limits, (c) total unit weight, (d) clay particle and fines content, (e) corrected cone resistance,  $q_t$ , (f) pore pressure,  $u_2$ , and (g) sleeve friction,  $f_s$  (from [5]).

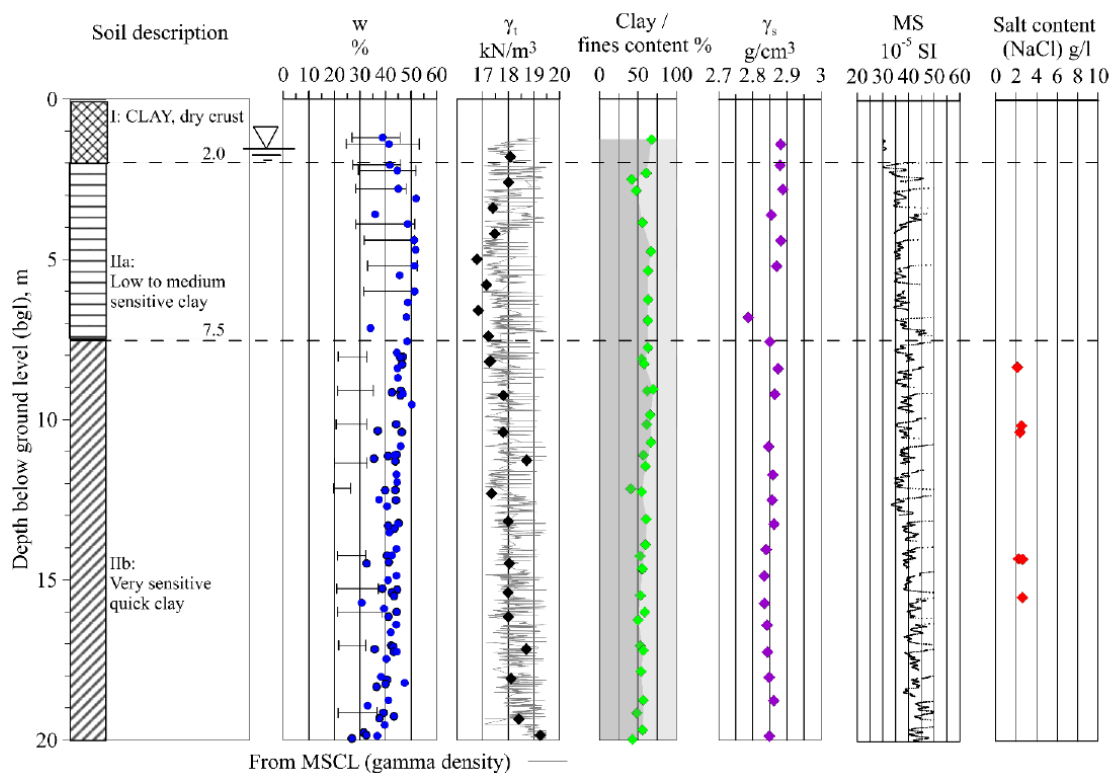


**Figure 2.4.** Basic soil profile, stratigraphy, and index properties at the Tiller-Flotten site.  $w$  = water content,  $\gamma_t$  = bulk unit weight,  $\gamma_s$  = particle density, and MS = magnetic susceptibility (From [4]).

### 2.3. Tiller high sensitivity site

Deposits of sensitive marine clay are found over large areas of Norway, Sweden, Finland, and North America. Such deposits are extremely challenging to deal with. In particular, quick clay deposits are frequently associated with landslides triggered by natural or man-made events. The Norwegian quick clay site, called Tiller, is near Trondheim (Figure 1.1). The soil deposit at Tiller is rather homogeneous with index properties, as shown in Figure 2.4. CRS oedometer tests show that the clay is slightly overconsolidated ( $OCR \sim 1.7$  to  $2.3$ ) down to 20 m. Quick clay has been identified between depths of about 3 to 20 m over the investigation area. The sensitivity of the clay was measured as high as 224, as the remoulded undrained shear strength can be as low as 0.1 kPa.

Figure 2.5 shows the results of CPTUs using 8 types of cone penetrometers. As was the case in the Onsøy and Halden sites, it can be seen that the results of  $q_t$  and  $u_2$  are quite consistent while there is quite a spread in the  $f_s$  data.

More details on the Tiller site are found in [4].

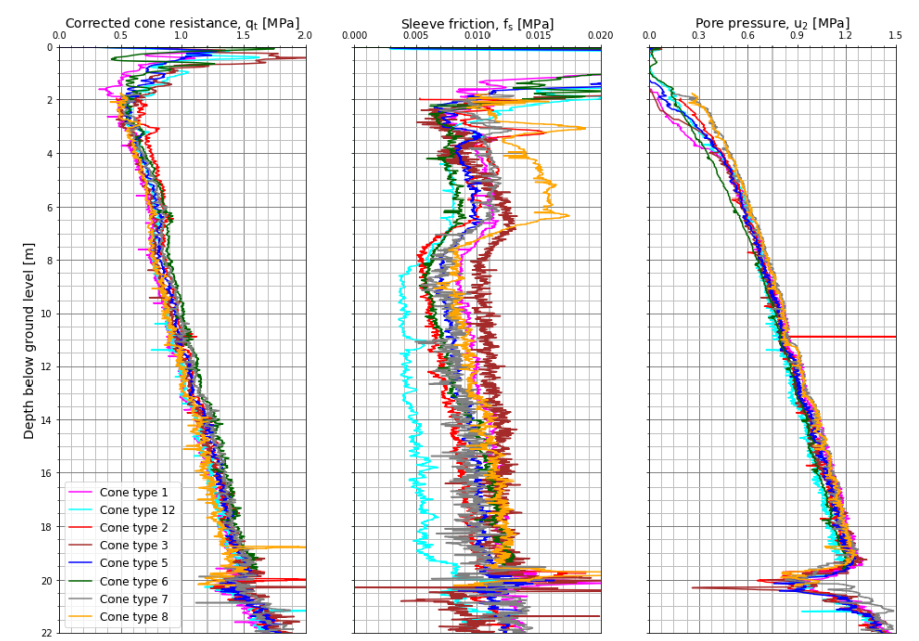


**Figure 2.5.** CPTU parameters for all cone types used at the Tiller site (from [11]).

### 2.4. Øysand sand site

The Øysand sand site is about 15 km southwest of Trondheim (Figure 1.1) and consists of a glaciofluvial deposit approximately 20 m thick. Site topography comprises a practically flat surface that lies at around 2.7 m above sea level, except for a 7 m high ridge along the south part of the field, which was created by the meandering nearby Gaula river ([12]). The sand layer is relatively homogeneous and consists mostly of fine to medium uniform sand with predominantly quartz minerals, some plagioclase, and micas. Characterization of the Øysand site included geophysical (electrical resistivity test, ERT, ground penetrating radar, GPR, and multichannel analysis of surface waves



(MASW)) and geotechnical (total sounding, SCPTU, SDMT, and slug test) investigations. Samples were obtained using fix piston samplers (Geonor-NGI, thin-walled open piston, and Gel Push sampler), and ground freezing. Series of laboratory tests, including monotonic drained and undrained triaxial tests, were performed on all available samples. For reference, a borehole log, close to where the piston samples were obtained, is shown in Figure 2.6.

CPTU test results are shown in Figure 2.7. More details are found in [6].

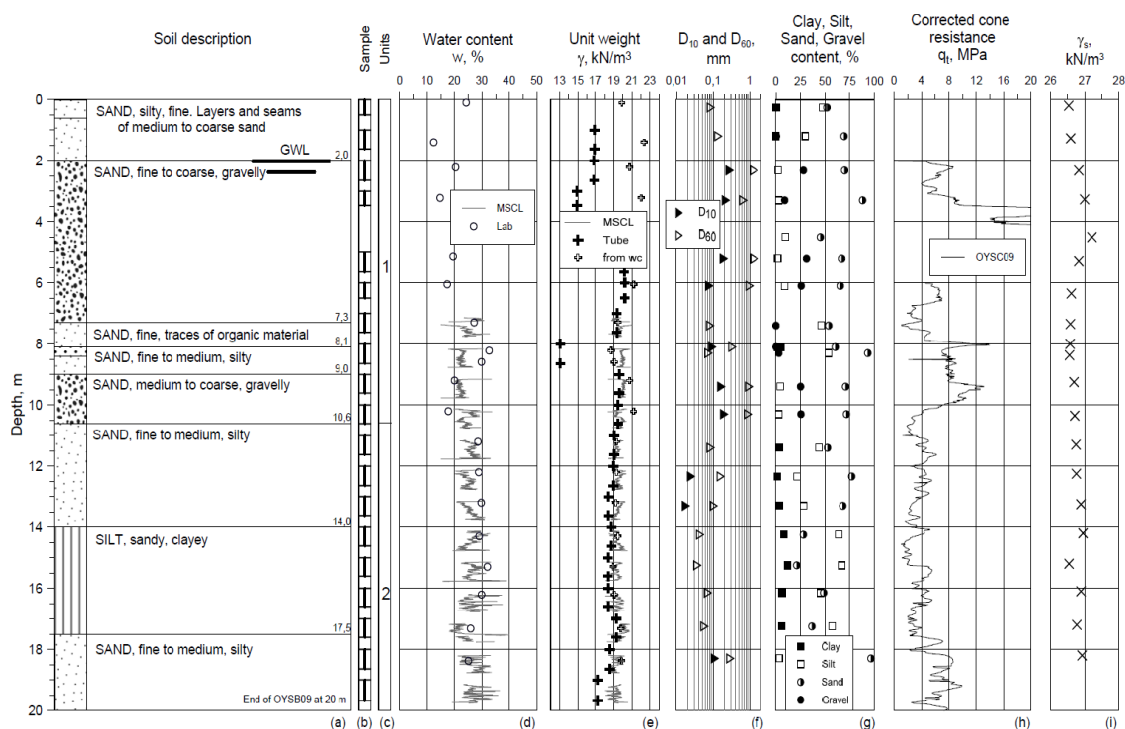


**Figure 2.6.** Borehole log (OYSB09). \* Multi sensor Core Logging [6].

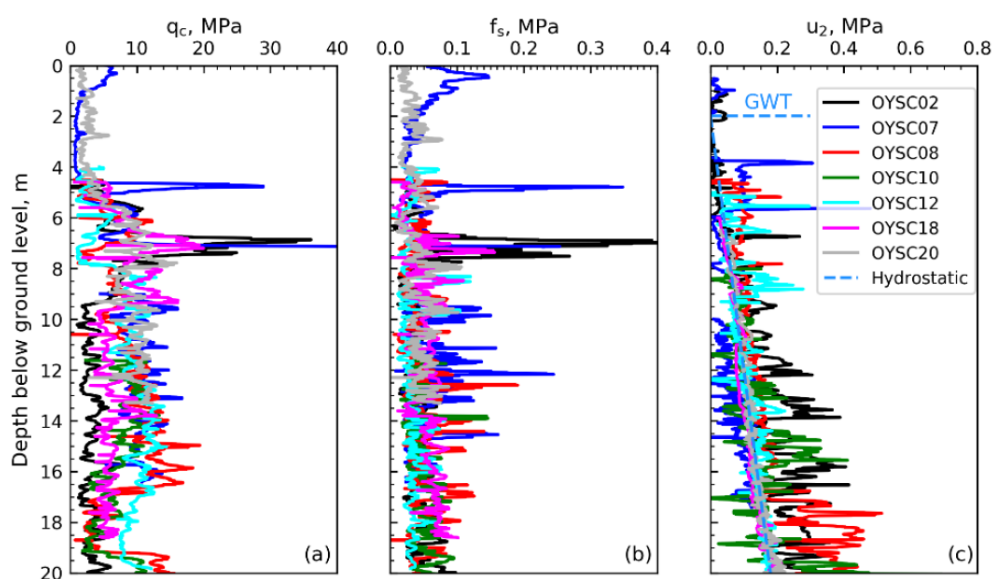


**Figure 2.7.** Results of seven CPTUs at Øysand (from [6]).

### 3. Overview of correlations used

#### 3.1. Introduction

The following correlations for evaluating soil parameters are covered in this paper:

- Soil unit weight,  $\gamma_t$  (all soils)
- Overconsolidation ratio, OCR (not for sand and silt)
- In situ lateral stress ratio,  $K_0$  (not for sand)
- Undrained shear strength corresponding to Anisotropic Consolidated Undrained Compression (CAUC) triaxial test,  $s_{uC}$  (not for sand)
- Peak friction angle from Anisotropic Consolidated Drained Compression (CADC) and CAUC,  $\phi_p$  (sand only)
- Shear wave velocity,  $V_s$  (all soils)
- Small strain shear modulus,  $G_{max}$  (or  $G_0$ ) (for all soils)

When using the correlations in the following section, it is assumed that results of only CPTU parameters  $q_t$ ,  $f_s$ , and  $u_2$  are available, and if SCPT is used, also  $V_s$ . Some correlations that also need soil index parameters like plasticity index or void ratio are not included.

In general, the correlations below are used by practitioners for all soil types, but often, the original authors' have stated that some soil types are excluded (where possible this is mentioned in the correlations below). Therefore, the use of certain correlations requires the engineer to know (or guess) the soil type, which often is not the case at an early stage and is regularly highly overlooked.

#### 3.2. Soil unit weight, $\gamma_t$

##### 3.2.1. Correlation No. 1 by [13] based on [14] SBT.

This approach consists of first defining the soil zone based on SBT charts (see Figure 3.1):

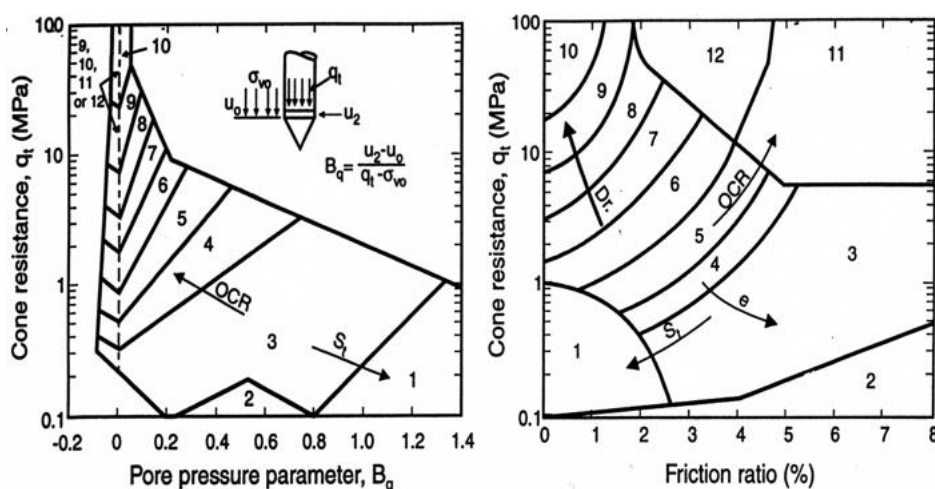


**Figure 3.1.** Soil Behaviour Type Classification Chart (SBT from [14])



If the two charts give different Zones, it is recommended to use the one you have most experience with and then choose a soil unit weight value from the following table (Table 3.1) given by [13]:

**Table 3.1.** Soil unit weight in kN/m<sup>3</sup>.

Zone	kN/m <sup>3</sup>
Zone 1 (sensitive soils)	17.5
Zone 2 (organics)	12.5
Zone 3 (CLAY)	17.5
Zone 4 (silty CLAY to CLAY)	18.0
Zone 5 (clayey SILT to silty CLAY)	18.0
Zone 6 (sandy SILT to clayey SILT)	18.0
Zone 7 (silty SAND to sandy SILT)	18.5
Zone 8 (SAND to silty SAND)	19.0
Zone 9 (SAND)	19.5
Zone 10 (gravelly SAND to SAND)	20.0
Zone 11 (very stiff fine grained)	20.5
Zone 12 (SAND to clayey SAND)	19.0

### 3.2.2. Correlation No. 2 by [15]

The authors of [15] suggested that the  $q_t$  vs  $R_f$  (friction ratio, calculated as the ratio between  $f_s$  and  $q_t$  given in %) chart in Figure 3.1 could be combined with Table 3.1, as shown in Figure 3.2, and that the contours of soil unit weight can be approximated using the following simplified equation:

$$\gamma_t = \gamma_w [0.27 \log R_f + 0.36 \log \left( \frac{q_t}{\sigma_{atm}} \right) + 1.236]$$

The researchers in [15] presented a database with 18 international sites covering a range of soil conditions and showed that, in general, their correlation works well.

### 3.2.3. Correlations No. 3 by [16] and [17]

Based on soil data from 115 sites offshore and onshore, as shown in Figure 3.3, the researchers in [16] developed the average correlation:

$$\gamma_t = \gamma_w [1.22 + 0.345 * \log (100 * (\frac{f_s}{\sigma_{atm}})) + 0.010]$$

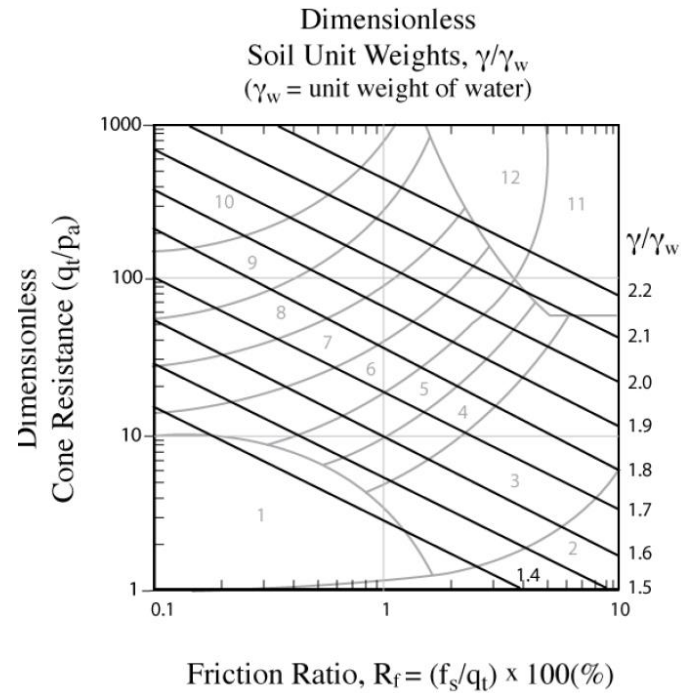


**Figure 3.2.** Relationship between CPT results and soil unit weight as proposed by [15].

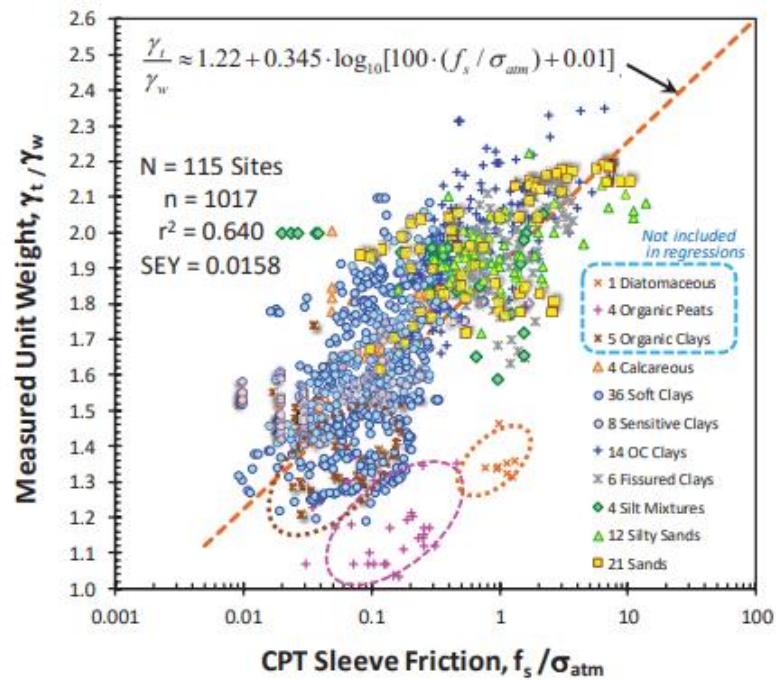


**Figure 3.3.** Total soil unit weight vs sleeve friction after [17].

Note that this correlation is based on the measured  $f_s$  only, and the scatter is large. The authors stress that the correlation is not applicable for organic clays, peats, and diatomaceous soils.

### 3.2.4. Correlation No. 4a and 4b by [18]

Based on shear wave velocity,  $V_s$  and soil data from a large a large number of international sites covering a wide range of soil conditions (Figure 3.4), Mayne suggested the following correlation (referred in this paper as correlation no. 4a) valid for uncemented soils (sands, silts, and clays):

$$\gamma_t = 8.31 * \log V_s - 1.61 * \log z$$

where  $V_s$  in (m/s), and depth  $z$  in (m) below the ground level.

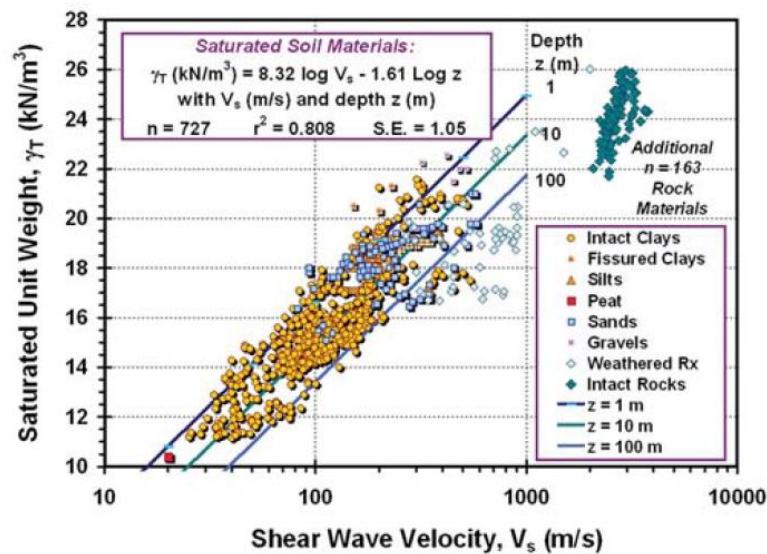


**Figure 3.4.** Saturated soil unit weight evaluation from shear wave velocity and depth (from [18]).

Based on  $V_s$  data to take into account effects of groundwater conditions through the effective stress-normalised shear wave velocity Mayne also suggested the normalised version (referred in this paper as correlation no. 4b) [18]:

$$V_{s1} = V_s / \left( \frac{\sigma'_{v0}}{\sigma_{atm}} \right)^{0.25}$$

$$\gamma_t = 4.17 * \ln V_{s1} - 4.03$$

this approach requires an iterative procedure between  $V_{s1}$  and  $\gamma_t$ )

### 3.3. Overconsolidation Ratio, (or Yield Stress Ratio) $OCR(= YSR) = \sigma'_p / \sigma'_{v0}$

#### 3.3.1. Correlations No. 5a, b by [19,20]

For intact inorganic clays with low sensitivity, the researchers in [19,20] suggested using simplified correlations for preconsolidation stress,  $\sigma'_p$ , based on statistical studies from 206 sites:

$$\text{Correlation no. 5a: } \sigma'_p = 0.33(q_t - \sigma_{v0})$$

$$\text{Correlation no. 5b: } \sigma'_p = 0.54(u_2 - u_0)$$

where all variables should have the same units, e.g., kPa for  $q_t$ ,  $u_2$ ,  $\sigma_{v0}$ , and  $u_0$ .

The effective cone resistance  $q_E = q_t - u_2$  can also be used to evaluate the preconsolidation stress [19,20]. This correlation is not used so much and is not included in the following assessment.

### 3.3.2. Correlations No. 6 by [21] and [22]

Based on the concept SHANSEP [23], the researchers in [21] suggested the following:

$$(Q_t)^{1-m} = S * N_{kt} * k_{OCR}^m$$

where  $OCR = k_{OCR}^m * Q_t$  when  $Q_t < 20$ ; where  $k_{OCR}^m$  and  $Q_t$  are dimensionless  $Q_t = (q_t - \sigma_{v0}) / \sigma_{v0}$ ,

$$s_u / \sigma'_{v0} = \frac{Q_t}{N_{kt}} = S * OCR^m;$$

where  $s_u$ ,  $\sigma'_{v0}$  are in kPa and  $Q_t$  and  $N_{kt}$  and  $S$  are dimensionless.  $S = (s_u / \sigma'_{v0})_{OCR=1}$  and  $m$  is a soil constant, function of soil behaviour type,  $I_c$  ( $m = 0.72$  in young, uncemented silica sands,  $m = 1$  when  $I_c > 2.8$  and  $m = 1 - [0.28 / (1 + I_c / 2.6)^{15}]$  when  $I_c \leq 2.8$ ).

The researchers in [22] then argued that for most sedimentary clays, silts, and organics, fine-grained soil,  $S \sim 0.25$ , for average direction of loading and  $\phi' \sim 26$ , and  $m \sim 0.8$ . Hence, the constant to estimate OCR can be automatically estimated based on CPT results using:

$$k_{OCR}^m = \left[ \frac{(Q_t)^{0.2}}{0.25 * (10.5 + 7 \log F_r)} \right]^{1.25}$$

then,  $OCR = (2.625 + 1.75 * \log F_r)^{-1.25} * Q_t^{1.25}$ .

Correlation no. 6 is used in section 4.

### 3.4. In Situ Stress Ratio (or Geostatic Stress Ratio), $K_0 = \sigma'_{h0} / \sigma'_{v0}$

#### 3.4.1. Correlation by No. 7a, b [24]

Based on a database with 12 intact and 5 fissured clays where in situ lateral stress ratio,  $K_0$ , were assessed using self-boring pressuremeter tests (Figure 3.5), the researchers in [24] suggested the following correlation (referred in this paper as correlation no. 7a):

$$K_0 = 0.1 \frac{q_t - \sigma_{v0}}{\sigma'_{v0}}$$

where all variables should have the same units, e.g., kPa for  $q_t$ ,  $\sigma_{v0}$  and  $\sigma'_{v0}$ .

For low plastic fine-grained soils, the researchers in [24] also suggested that if OCR has been assessed by CPTU data, the following approximate correlation may be used (referred in this paper as correlation no. 7b):

$$K_0 = 0.5 * OCR^{0.5}$$

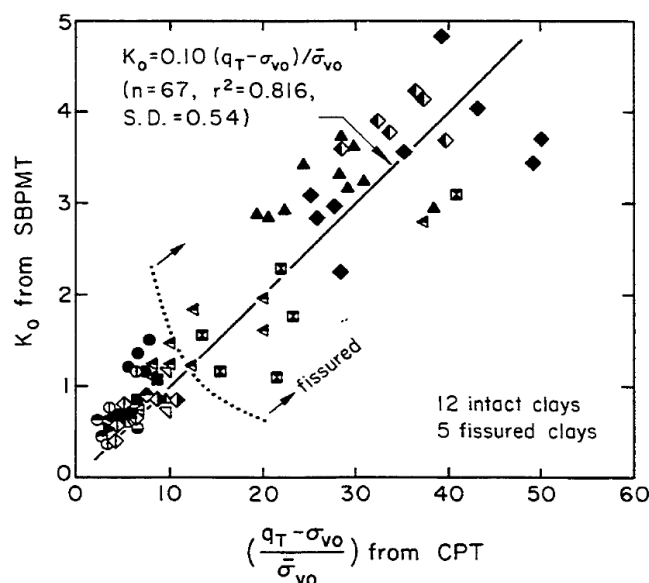


**Figure 3.5.** Correlation between  $K_0$  from SBPMT and normalised  $q_t$  (from [24]).

### 3.5. Undrained shear strength, $s_u$

To evaluate  $s_u$  from net cone resistance, the  $q_{net}$  value in the following well-known equation (see e.g., [13]) was used:

$$s_u = \frac{q_t - \sigma_{v0}}{N_{kt}}$$

Another approach is to evaluate  $s_u$  from excess pore pressure ( $u_2 - u_0$ ), using the following equation (see for instance [25] and [13]):

$$s_{uC} = \frac{u_2 - u_0}{N_{\Delta u}}$$

where  $u_0$  is in situ static pore pressure.

To determine the cone factors,  $N_{kt}$  (or  $N_{\Delta u}$ ) and the following correlations (from no.8 to no. 10) are used, and the results are presented and discussed in sections 4 and 5.

#### 3.5.1. Correlation No. 8 by [22]

The researchers in [22] argued that since  $N_{kt}$  is strongly influenced by sensitivity, the following expression may be used to evaluate  $N_{kt}$ .

$$N_{kt} = 10.5 + 7 \log F_r$$

No database is referred to back up this correlation; neither is it mentioned which type of  $s_u$  is the reference.

### 3.5.2. Correlation No. 9 by [26]

Based on data from a large number of onshore and offshore clays, the researchers in [26] established a correlation, as shown in Figure 3.6. The reference  $s_u$  is that measured in a triaxial test where the specimen has been consolidated to best estimate in situ stresses and sheared in compression, i.e.,  $s_{uc}$ . It is suggested that the  $N_{kt}$  value can be assessed from the pore pressure ratio,  $B_q$  value, as measured in a CPTU.

$$N_{kt} = 10.5 - 4.6 \ln(B_q + 0.1)$$

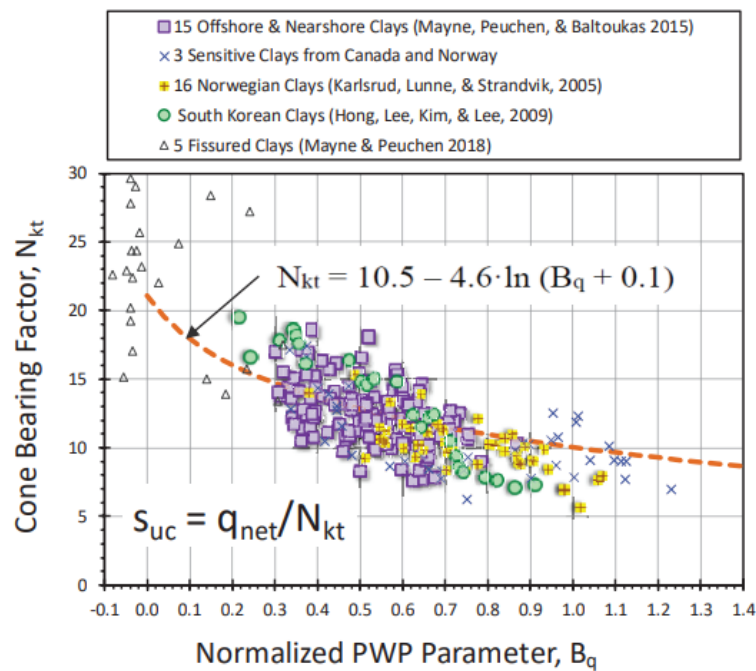


**Figure 3.6.** Data sets for establishing the  $N_{kt}$  relationship with  $B_q$  (from [27][26]).

### 3.5.3. Correlation No. 10 by [22]

Based on the fact that  $N_{\Delta u} = B_q * N_{kt}$ , and the correlation shown in Figure 3.6, the researchers in [22] suggested that as a conservative estimate,  $N_{\Delta u}$  could be determined by the following equation:

$$N_{\Delta u} = B_q * [10.5 - 4.6 \ln(B_q + 0.1)]$$

## 3.6. Peak friction angle, $\phi_p$

The peak friction angle,  $\phi_p$ , was calculated using two of the most common equations found in the literature as detailed below.

### 3.6.1. Correlation No. 11 by [24] in [22]

The relationship proposed by [24] for clean, rounded, uncemented quartz sands using high-quality, mostly frozen soil samples is:

$$\phi_p = 17.6 + 11 \log(Q_{tn})$$

where  $Q_{tn} = ((q_t - \sigma_{v0}) / \sigma_{v0}') \cdot (\sigma_{v0}' / \sigma_{atm})^n$ .

### 3.6.2. Correlation No. 12 derived from [28] in [22]

The proposed equation links the clean sand equivalent cone resistance,  $Q_{tn,cs}$ , and the constant volume friction angle,  $\phi_{cv}$ :

$$\phi_p = \phi_{cv} + 15.84 [\log(Q_{tn,cs})] - 26.88$$

Depending on mineralogy, typical values of  $\phi_{cv} = 33^\circ$  for sub-rounded quartz sands, and are as high as  $40^\circ$  for felspathic and carbonate sands.

### 3.6.3. Correlation No. 13 by [29]

The probabilistic study by [29] proposed an equation to estimate  $\phi$  based on shear wave velocity,  $V_s$ , in m/s using:

$$\phi_p = 3.9(V_{s1})^{0.44}$$

$$\text{where } V_{s1} = V_s / (\sigma_{v0}' / \sigma_{atm})^{0.25}$$

## 3.7. Shear wave velocity

Note that the shear wave velocity,  $V_s$ , from a seismic CPTU and a seismic DMT is vertically propagating and horizontally polarized shear wave ( $V_{s,VH}$ ), and is, hence, is only strictly comparable with a bender element test with a similar orientation (top to bottom) in the laboratory.

### 3.7.1. Correlation No. 14 by [30]

The researchers in [30] established a correlation between  $q_c$  and  $V_s$  ( $V_{hv}$ ), measured using cross-hole tests and seismic cone penetration tests performed from the sites of Po River sand and of the Gioia Tauro sand with gravel. Please, note that this correlation is valid only for cohesionless soils.

$$V_s = 277(q_t)^{0.13} \cdot (\sigma'_{v0})^{0.27}$$

where both  $q_t$  and  $\sigma'_{v0}$  in MPa.



### 3.7.2. Correlation No. 15 by [31]

Based on a database from 31 clay sites, the researchers in [31] suggested the following equation:

$$V_s = 31.4 \left( \frac{q_t}{\sigma_{atm}} \right)^{0.627} \text{ or}$$

$$V_s = 1.75(q_t)^{0.627} \text{ but in this correlation, } q_t \text{ in kPa.}$$

This reference also shows that if the voids ratio,  $e$ , is included, then the fit with the revised correlation is improved; however, as void ratio is an unknown parameter when progressing CPTU results, the equation has not been used here.

### 3.7.3. Correlation No. 16 by [32]

Based on extensive SCPT data, the researchers in [32] suggested the following relationship

$$V_s = \left( 10^{(1.68+0.55I_c)} * \left( \frac{q_t - \sigma_{v0}}{\sigma_{atm}} \right) \right)^{0.5}$$

## 3.8. Small Strain Shear Modulus, $G_0 = G_{max}$

### 3.8.1. Correlation No. 17 by [32]

The researchers in [32] used the above equation for  $V_s$  and an average soil unit weight of  $18 \text{ kN/m}^3$  to arrive at the following expression for  $G_0$ :

$$G_0 = (q_t - \sigma_{v0}) * 0.0188 * 10^{(0.55I_c+1.68)}$$

where  $q_t$  and  $\sigma_{v0}$  are in kPa.

## 3.9. Coefficient of permeability, $k_h$

### 3.9.1. Correlation No. 18 by [33]

The proposed relationship [33] between soil permeability,  $k_h$ , and SBT,  $I_c$ , shown in Figure 3.7 can be represented by:

$$k_h = 10^{(0.952 - 3.04I_c)} \quad \text{When } 1.0 < I_c \leq 3.27;$$

$$k_h = 10^{(-4.52 - 1.37I_c)} \quad \text{When } 3.27 < I_c < 4.0;$$

where  $k_h$  is in m/s; and  $I_c = ((3.47 - \log Q_t)^2 + (\log F_r + 1.22)^2)^{0.5}$ .

Based on the values of permeability,  $k_h$  in Table 3.2 for the zones defined in the SBT chart [33] simplified the relationship with  $I_c$  and  $k_h$ , as shown in Figure 3.7.

**Table 3.2.** Estimated soil permeability,  $k_h$ , based on a normalized CPT soil behaviour chart (modified from [13]).

SBTn Zone	SBTn	Range of $k$ (m/s)	SBTn $I_c$
1	Sensitive fine-grained	$3 \times 10^{-10}$ to $3 \times 10^{-8}$	NA
2	Organic soils - clay	$1 \times 10^{-10}$ to $1 \times 10^{-8}$	$I_c > 3.60$
3	Clay	$1 \times 10^{-10}$ to $1 \times 10^{-9}$	$2.95 < I_c < 3.60$
4	Silt mixture	$3 \times 10^{-9}$ to $1 \times 10^{-7}$	$2.60 < I_c < 2.95$
5	Sand mixture	$1 \times 10^{-7}$ to $1 \times 10^{-5}$	$2.05 < I_c < 2.60$
6	Sand	$1 \times 10^{-5}$ to $1 \times 10^{-3}$	$1.31 < I_c < 2.05$
7	Dense sand to gravelly sand	$1 \times 10^{-3}$ to 1	$I_c < 1.31$
8	*Very dense/ stiff soil	$1 \times 10^{-8}$ to $1 \times 10^{-3}$	NA
9	*Very stiff fine-grained soil	$1 \times 10^{-9}$ to $1 \times 10^{-7}$	NA

\*Overconsolidated and/or cemented

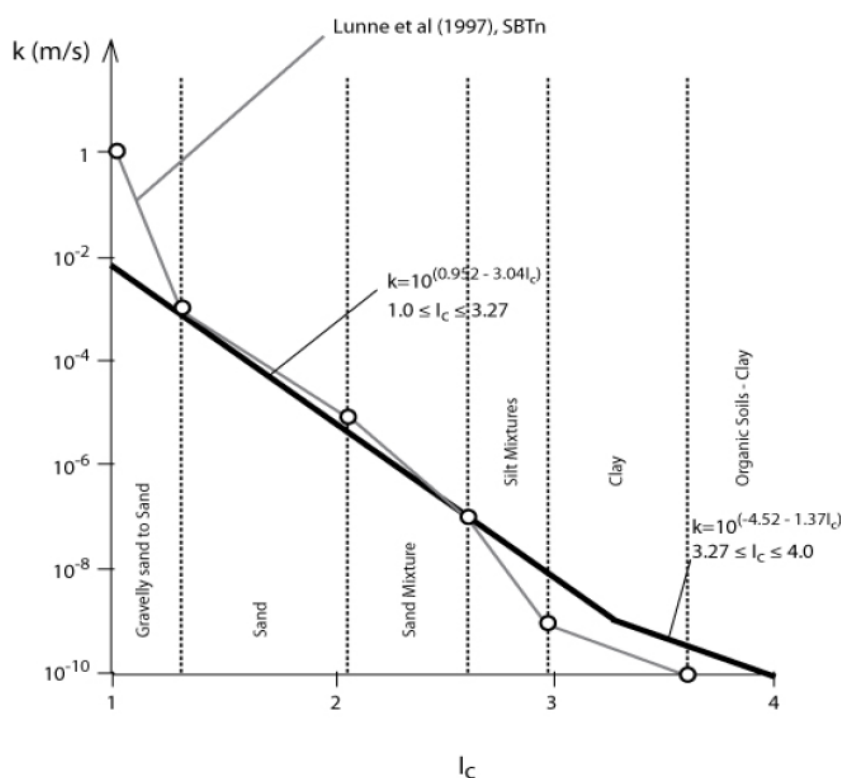


**Figure 3.7.** Suggested variation of soil permeability,  $k_h$ , as a function of SBT,  $I_c$ , from [33].

#### 4. Comparison of correlations and field or lab best estimates from the NGTS sites

##### 4.1. Soil unit weight, $\gamma$

Measured parameters from a CPTU test,  $q_c$ ,  $u_2$ , and  $f_s$  are used to directly calculate the corrected cone resistance,  $q_t$ . To further derive soil properties, using the measured data from CPTU test correlations require additional input parameters of which the two most important are soil unit wet

weight,  $\gamma$  and hydrostatic pressure or equilibrium pore water pressure,  $u_0$ , which often are not known at the time of CPTU data processing and reporting. To progress with soil property estimation, it is required to assume the hydrostatic pore water pressure, and local topography, ditches, etc. might well indicate where the exact ground water level is.

The measurements of the cone are affected by the soil density and in situ stresses and, therefore, several researchers have tried to link density to CPTU measurements. Many correlations have been proposed over the years to derive  $\gamma$  from CPTU/ SCPTU data and some are detailed in Section 3. Other correlations require the total or vertical effective stress in the soils, and this requires an estimation of  $\gamma$ . Using such correlations, an iteration procedure is needed, which complicates the calculations and adds another layer of uncertainties to the results. For this reason, to reduce uncertainties, only the correlations that require measured CPTU data are utilised in this paper.

Derived  $\gamma$  from  $q_t$ ,  $f_s$  and  $V_s$  measurements are compared with laboratory measurements of  $\gamma$  with the primary focus on results from high quality undisturbed samples (e.g., block samples in clay or ground freezing in sand). However,  $\gamma$  from other samples is also considered to increase the amount of data in this database.

Figure 4.1 presents  $\gamma$  results for the four sites described in section 2. It is seen that, from all correlations based on CPTU measurements,  $\gamma$  is always underestimated in comparison to laboratory results, although the profiles derived from CPTU data seem to show roughly the variation of  $\gamma$  with depth. When considering the correlations that utilise the shear wave velocity,  $V_s$ , it can be seen that these typically underestimate  $\gamma$  except at the quick clay site of Tiller. This underestimation of  $\gamma$  by the correlations has been shown to be true for other soil types, but it is occasionally overestimated ([34]).

An alternative approach is to use Table 3.1, which relates SBT from Robertson's soil identification charts with  $\gamma$ . If the normalised charts are used, then an iterative procedure must be adopted as  $\gamma$  is needed in the normalisation process. It can be seen in Figure 4.1 that this method appears to give sometimes a better assessment of  $\gamma$ , but it is rather crude and is more than likely to overestimate it in softer soils.

To emphasise the importance of using a correct  $\gamma$  in the estimation of soil properties from the CPTU tests, each additional parameter discussed in this paper is derived using the CPTU-based  $\gamma$  profile and the best estimate  $\gamma$  profiles from laboratory results.

Øysand results of  $\gamma$  are presented in two separate plots. Figure 4.1 (d) shows the  $\gamma$  obtained in the laboratory from fixed push piston samples compared against estimated  $\gamma$  values based on CPTU and  $V_s$  (from SCPTU and laboratory Bender elements). Figure 4.1 (e) compares  $\gamma$  measured on undisturbed samples obtained by ground freezing and estimated values based on CPTU and shear wave velocities from SDMT in the field and Bender elements in the laboratory. All estimates of  $\gamma$  in both cases were lower than the measured  $\gamma$  for samples from fixed piston and ground freezing. Nonetheless, fixed piston samples were obtained in a disturbed state ([35]) and may have been loosened during sampling, which may explain why such samples plot closer to the estimates. In contrast, values of  $\gamma$  on samples obtained by ground freezing are consistently and significantly higher than any of the estimates.

#### 4.2. Overconsolidation ratio, OCR (or YSR)

As we consider deriving geotechnical parameters, in this section, we discuss the estimation of the overconsolidation ratio, OCR. In the published papers for Onsøy by [3], and for Tiller by [4], the OCR

results derived from oedometers tests with constant rate of consolidation strain (CRS) show reduction with depth and are reported between 1.8–1.3 for Onsøy and 2.3–1.7 for Tiller. For the Halden site, OCR is not included due to the unclear definition of OCR from CRS tests. Also, for Øysand site OCR is not included as no CRS tests have been yet performed on undisturbed sand.

It can be seen in Figure 4.2 that the three correlations explained in Section 3.2 using the derived  $\gamma$  give a significant range of estimated OCR for both test sites. There is no consistent pattern between them. For Onsøy, two of the correlations appear almost acceptable with the third one being significantly higher. When the best estimate  $\gamma$  from laboratory tests on block samples is used, the pattern changes significantly with this high value correlation, from Figure 4.2a now giving the best fit in Figure 4.2b. For Tiller, all three correlations significantly overestimate OCR. However, all correlations show the right trend of decreasing OCR with depth. When using the best estimate  $\gamma$  profile, the pattern of results improves with one correlation now almost fitting in Figure 4.2(d).

The OCR correlations explained in Section 3 need constants that are soil dependent. Establishing site specific constants can significantly improve OCR results. Looking at Onsøy, if the constant in [19] correlation, which uses net cone resistance,  $q_{\text{net}}$ , is changed from 0.33 (which is the global value in the literature suggestion) to 0.5, then the agreement is significantly improved. For Tiller, if constants in both correlations are changed from 0.33 (in the correlation that uses the  $q_{\text{net}}$ ) and 0.54 (in the correlation that uses the excess pore pressure,  $u_2 - u_0$ ) to 0.3 and 0.4, respectively, the agreement would be much more satisfactory. This shows that the correlations need to be related to site specific conditions. However, OCR is a parameter that needs special care and good knowledge of the geological history of the sites when estimated from the CPTU-based correlations.

OCR has been used here because it is more commonly used, but it may be better in the future to use the correlations for yield stress because the vertical effective stress does not need to be estimated.

#### 4.3. Lateral stress ratio, $K_0$

$K_0$  is difficult to establish in the laboratory regardless of the quality of samples. However, it can be best measured in situ using self-boring pressuremeter tests (SBP). In two of the sites (Halden and Onsøy), pressuremeter tests were performed in the vicinity with CPTU tests. Therefore, measured  $K_0$  profiles from SBP were compared with the derived profiles from CPTU tests using the correlations mentioned in Section 3.4. When using the CPTU derived  $\gamma$ , there is a significant scatter in the results. However, the results agree very well for the soils encountered in Halden when using the best estimate  $\gamma$  profiles.

For Onsøy, to improve the agreement between the CPTU derived  $K_0$  and the in situ measured  $K_0$ , the constant used in [24] needs to change for a correlation from 0.1 for the whole soil profile to 0.2 in soils encountered in the top 10.5m and 0.15 for the rest of the soil profile (Figure 4.3). These results again prove the need for site specific constants to be used in the CPTU-based correlations for deriving  $K_0$ .

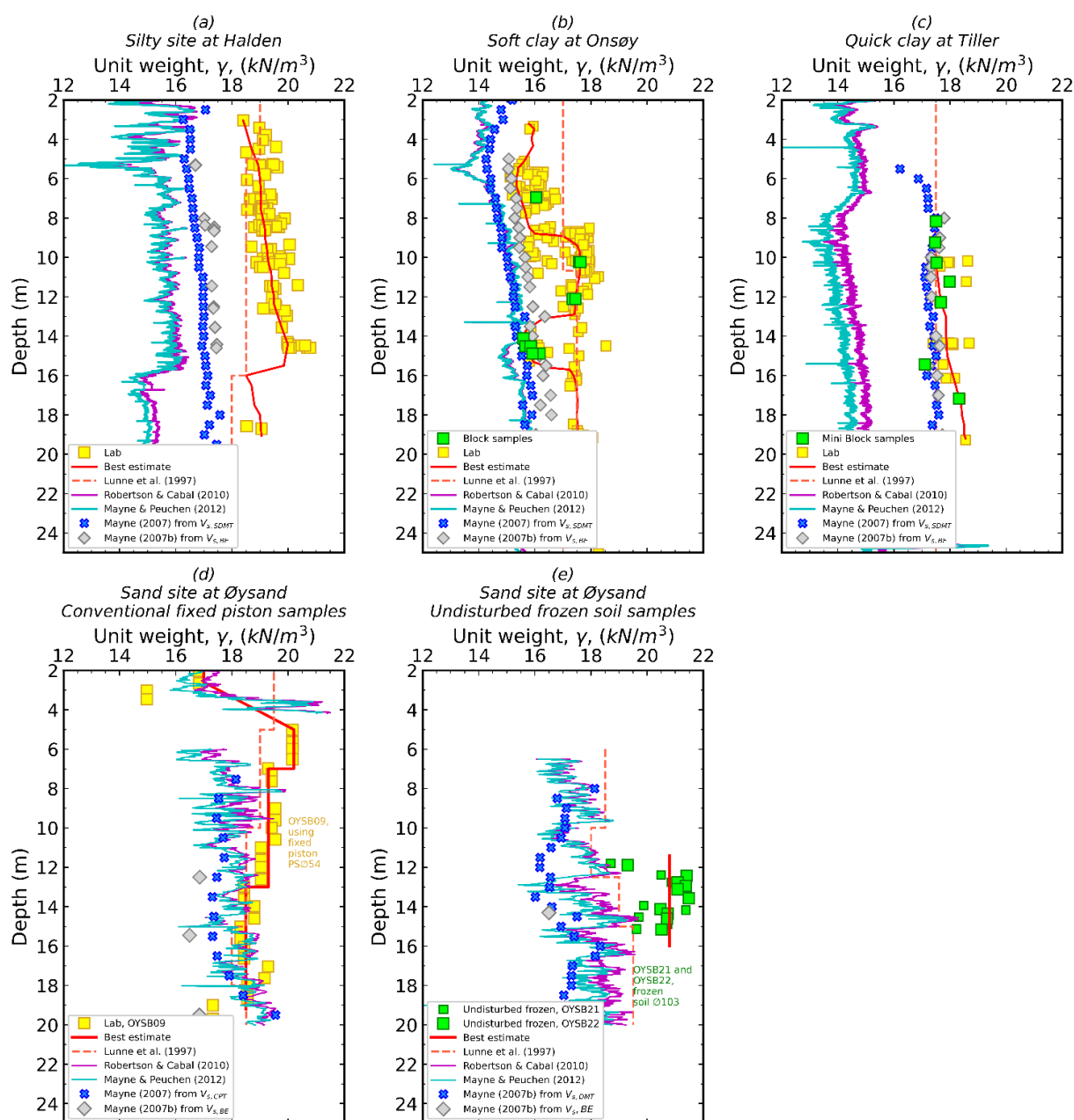


**Figure 4.1.** Laboratory and CPTU/ $V_s$ -estimated  $\gamma$  profiles for: (a) silty site at Halden, (b) soft clay at Onsøy, (c) quick clay at Tiller, (d) sand at Øysand piston samples, and (e) Øysand ground freezing for sampling.

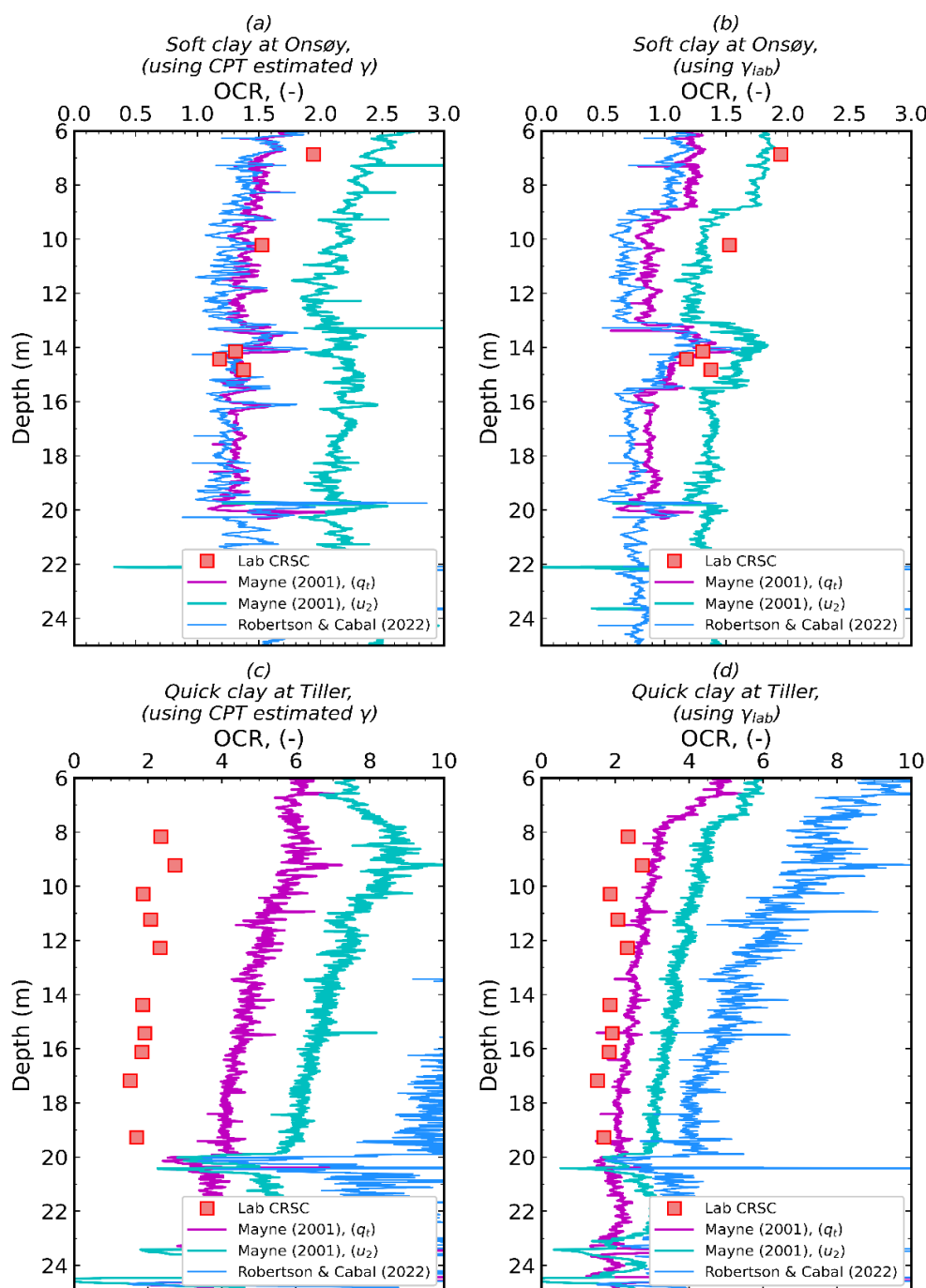


**Figure 4.2.** OCR profiles for: (a) Soft clay at Onsøy using the CPTU-derived  $\gamma$ , (b) soft clay at Onsøy using the best estimate  $\gamma$  profile from laboratory measurements, (c) quick clay at Tiller using the CPTU-derived  $\gamma$ , and (d) Quick clay at Tiller using the best estimate  $\gamma$  profile from laboratory measurements (CRSC in the legend refers to oedometer results on block samples).

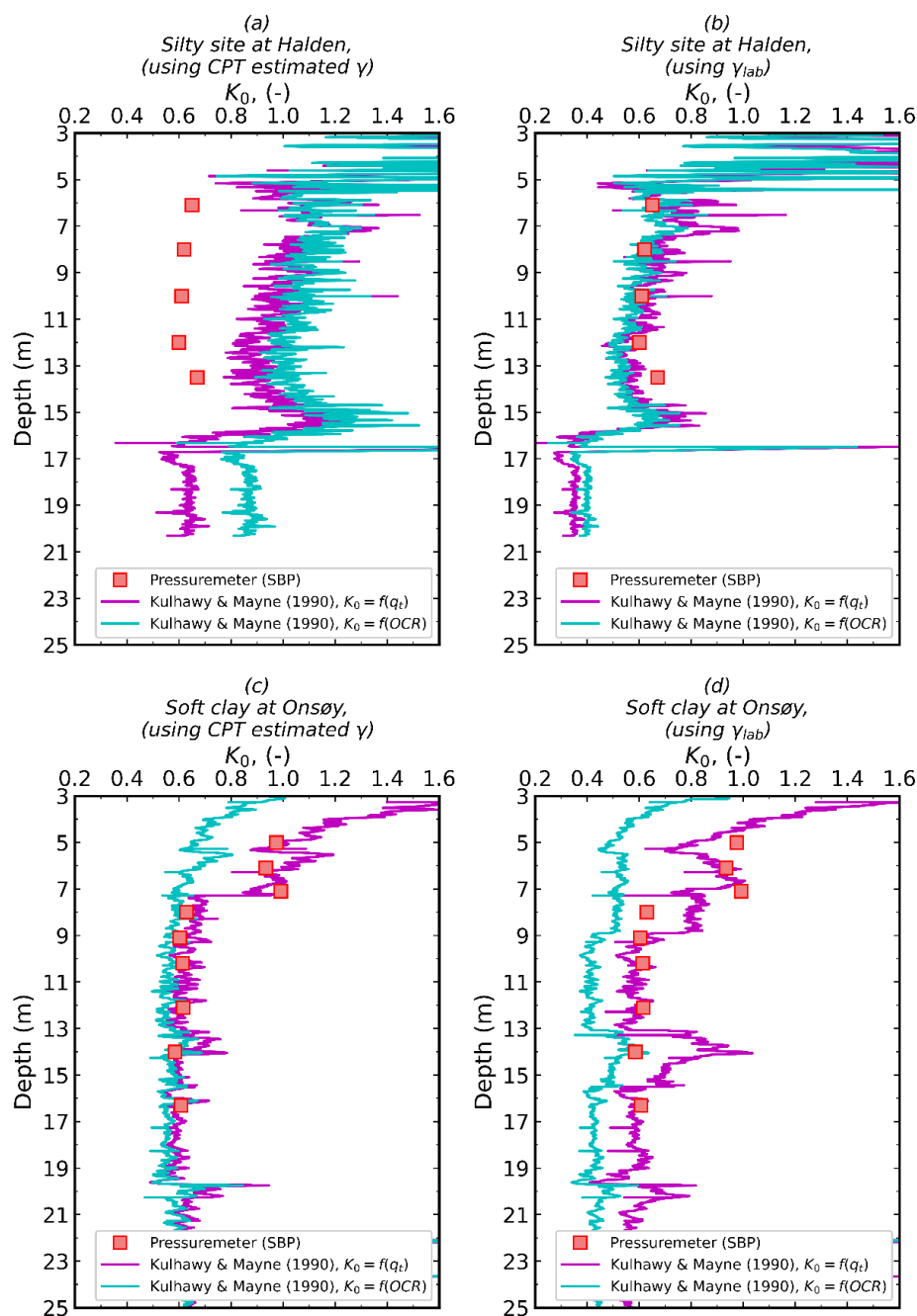


**Figure 4.3.**  $K_0$  profiles for: (a) Silty site at Halden using CPTU-based derived  $\gamma$ , (b) silty site at Halden using the best estimate  $\gamma$  from laboratory measurements, (c) soft clay at Onsøy using CPTU-based derived  $\gamma$ , and (d) soft clay at Onsøy using the best estimate  $\gamma$  profile from laboratory measurements.

#### 4.4. Undrained shear strength, $s_u$

Undrained shear strength is probably the most commonly derived parameter from CPTU measurements and is highly impacted by the cone factor,  $N_{kt}$  (or  $N_{\Delta u}$ ). Furthermore, the number of correlations to derive  $s_u$  and  $N_{kt}$  (or  $N_{\Delta u}$ ) that are available in the literature is high. In fact, some



software packages have inbuilt equations for deriving  $N_{kt}$  or  $N_{\Delta u}$ , but only those mentioned in Section 3.5 are considered here as examples. There are several ways to reach to the  $N_{kt}$  or  $N_{\Delta u}$  values, but the most accurate one is to back calculate the cone factors from CAUC triaxial tests on high quality samples. Also, previous experiences and knowledge of soil conditions is helpful. Literature recommendations on guidance values for the cone factors on various soil deposits can be helpful when the first 2 methods are not possible. It is not uncommon to take a range of typical values for  $N_{kt}$  or  $N_{\Delta u}$  to derive shear strengths.  $N_{kt}$  values of 15 and 20 are often taken, and for  $N_{\Delta u}$ , a value of 10 is most common (where  $N_{\Delta u} = B_q \cdot N_{kt}$ ). Note that the most erroneous way of deriving  $s_u$  is by using the default values of cone factors preassigned in the software packages. A range of  $N_{kt}$  from 15 to 25 for all soil types can result in highly unrealistic values for certain deposits. However, it is worth mentioning that in some cases, cone factors cannot be one single value representative for the whole profile regardless of how homogeneous these soils may be. The test sites are considered highly homogeneous sites and well characterised over the years. Yet, at Onsøy, there is a layer between 14.0–15.5 m that shows deviation from representative layer values for  $w$  and  $\gamma$  laboratory results, which is also followed by higher values of  $s_u$ . In this case back calculating  $N_{kt}$  only for this sublayer led to a cone factor of 8.

As mentioned, the values quoted above are those back-calculated from tests on block samples. However, if it was desirable to link with samples obtained by other methods as based on historical experience, then it can be seen that the CAUC tests on block samples at upper meters at Onsøy are lower and, therefore, to match these results, the values of a cone factor would need to be higher. Figures 4.4 (a, c, e) show  $s_{uC}$  using CPTU-based derived  $\gamma$  for the three  $N_{kt}$  and  $N_{\Delta u}$  correlations. For Halden and Tiller, the correlations based on  $B_q$  works reasonably well, while the one based on  $F_r$  overestimates the strength significantly. For Onsøy, the correlations based on  $F_r$  significantly underestimates the strength, while the ones based on  $B_q$  work slightly better. For  $s_{uC}$ , the potential errors in using CPT-derived  $\gamma$  is quite small since  $\gamma$  is used to only calculate  $\sigma_{v0}$  for getting  $q_{net} = q_t - \sigma_{v0}$ . This is illustrated in Figure 4.4 (b, d, f), where  $s_{uC}$  has been calculated with various  $N_{kt}$  values. Looking at these Figures, we would be looking at  $N_{kt}$  values of around 15 for Halden of around 9 for Onsøy and around 10 for Tiller. The latter two are significantly below the typical assumed range of 15–20 mentioned earlier, which would have underestimated to shear strengths.

#### 4.5. Peak friction angle, $\phi_p$

The triaxial peak friction angle, obtained from CADC and CAUC tests, are presented and compared against the  $\phi_p$  estimated from CPTU and shear wave velocity measurements ( $V_s$  measured with SCPTU, MASW, or SDMT). Two sets of tests are presented in Figure 4.5; one is based on triaxial samples obtained using a fixed piston sampler (close to CPTU OYSC09, using a Geonor PSØ54 with composite liner) and a second dataset on triaxial test results from undisturbed samples obtained by ground freezing (sampled ca. 10 m from CPTU OYSC20). In both figures, comparisons are made against estimations obtained using [24] (K&M), [22] (R&C) and [29] equations. There is no unique trend or best equation to estimate  $\phi_p$ . In general,  $\phi_p$  values from fixed piston samples are lower than the results for frozen specimens, though estimations seem to be able to predict  $\phi_p$  of the frozen samples and underestimate it in the case of fixed pistons. Note that the R&C equation is directly influenced by the choice of  $\phi_{cv}$ . In Figure 4.4(a), the value of  $\phi_{cv} = 33^\circ$  was assumed; if, for instance,  $\phi_{cv} = 36^\circ$  was

used instead, the equation conveys towards K&M estimations. The  $\phi_p$  estimated from  $V_s$  results in fair approximations, though discrepancies may arise from the lateral and vertical soil variability and from the fact that  $V_s$  was not continuously measured.

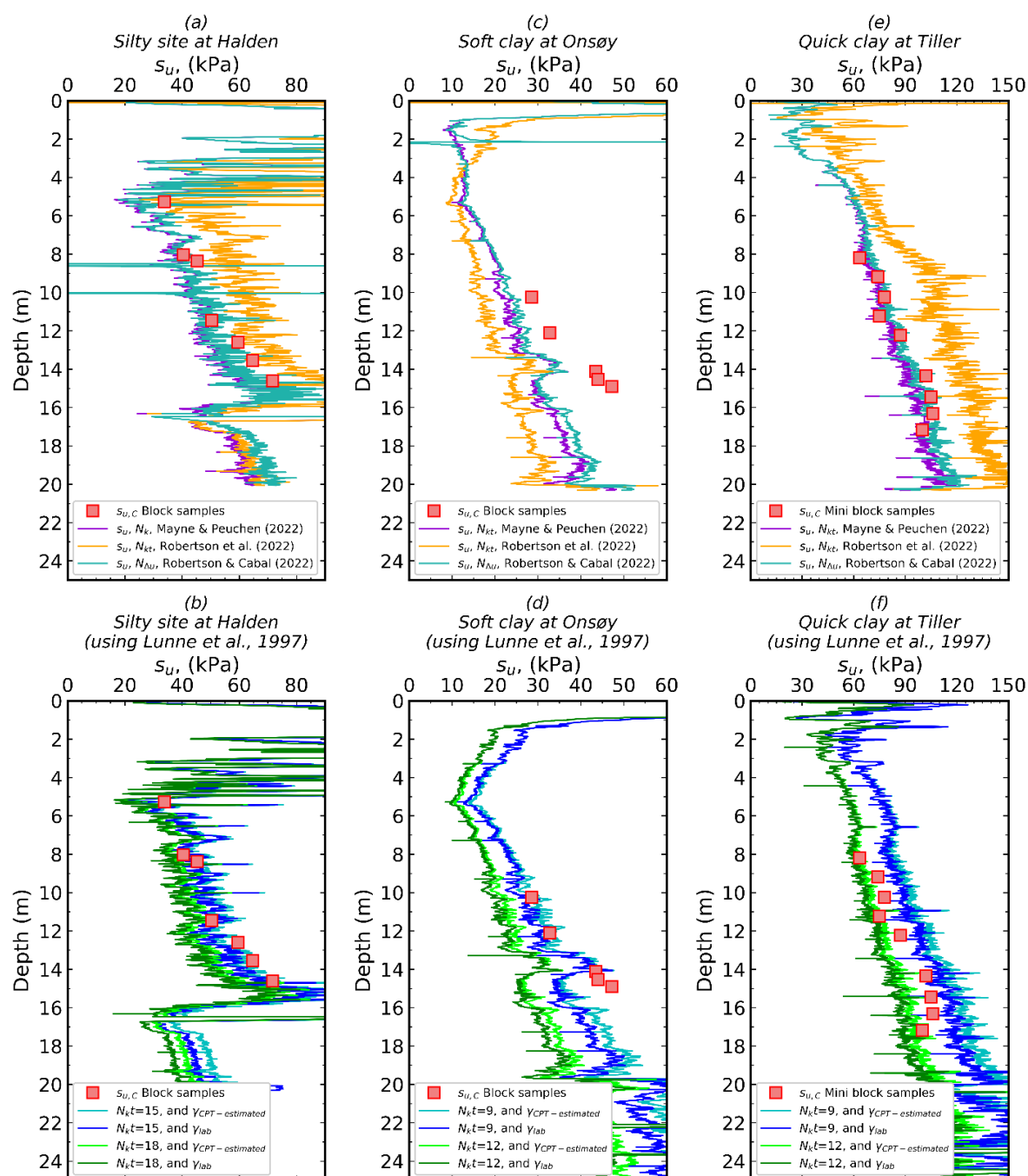


**Figure 4.4.**  $s_u$  profiles for: (a) and (b) Silty site at Halden, (c) and (d) soft clay at Onsøy, and (e) and (f) quick clay at Tiller.

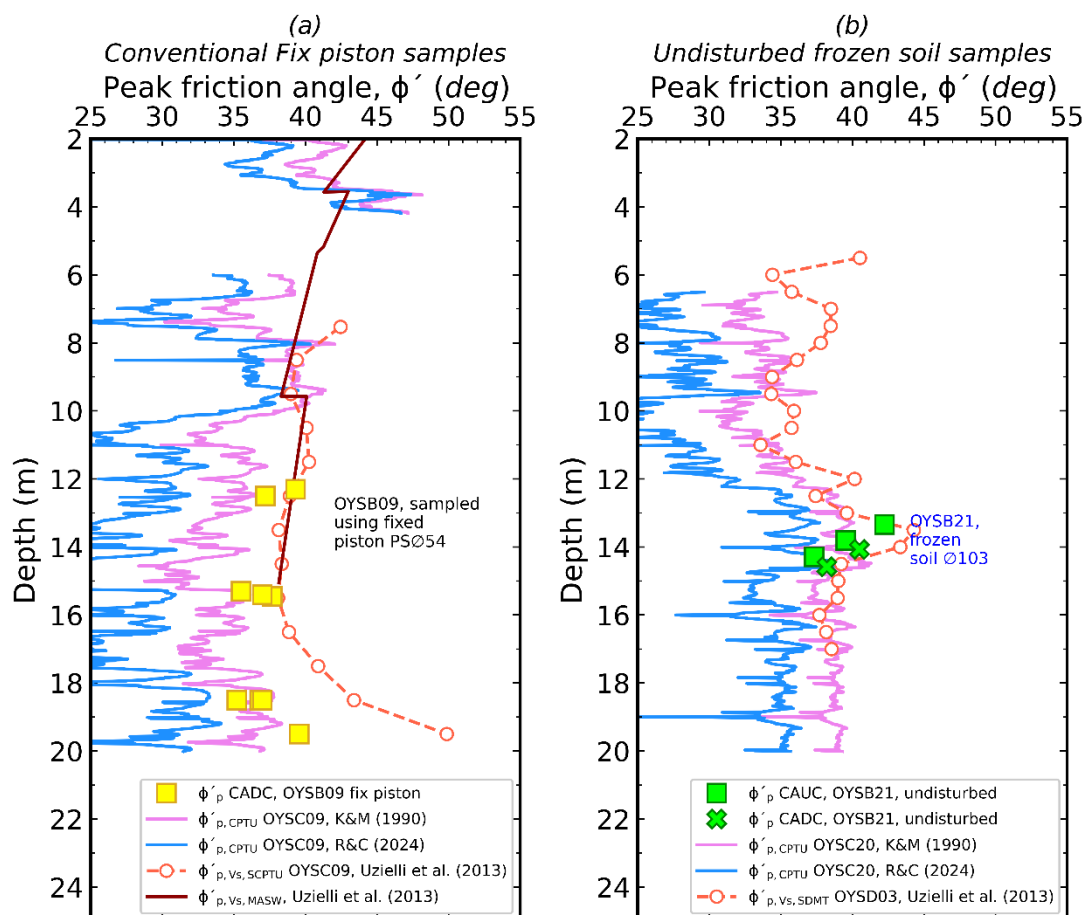


**Figure 4.5.** Friction angle from triaxial tests on (a) fixed piston samples and (b) undisturbed frozen sand samples compared against estimations based on CPTU and  $V_s$ .

#### 4.6. Shear wave velocity, $V_s$

Shear wave velocity is one of the parameters that can easily be measured on site. The best way to generate accurate  $V_s$  profiles is to take measurements at least every 1m using a seismic probe (either seismic CPTU or seismic DMT, with dual receivers). However, various correlations are published on how to derive  $V_s$  profiles from CPTU measurements. Some of the widely used correlations are discussed in Section 3.6. Figure 4.6 shows the results obtained using these correlations at all four sites.

Figure 4.6 (g and h) shows the  $V_s$  profiles at Øysand measured with MASW, SCPT, and BE in the laboratory for samples obtained with a fixed piston sampler at the OYSB09 borehole. Estimations of  $V_s$  from [30] and [32] equations are lower than SCPTU measurements and fit with MASW and BE measurements. Nonetheless, BE measurements are believed to be conservative estimates, as those were obtained on rather disturbed samples.

It was observed that there was a lot of scatter in the derived results. Unfortunately, to add more confusion, when the best estimate values for  $\gamma$  are used as an input, the scatter becomes more pronounced. Initially, the results appear to be in agreement when processing using generated estimates of  $\gamma$ , though they are wrong when true unit weights are used, which is very worrying if used for designs without knowledge on the site conditions, advanced laboratory results, and critical engineering

judgement. It might be pondered why we guess  $V_s$  using correlations when it can be measured. Adding to the work of the researchers in [36] on correlations of  $G_0$  with cone results and orientation of measurements, the researchers in [37] showed that cone measurements may well relate better to horizontal shear wave velocities than vertical; thus, it is questioned why a common correlation should work for  $V_s$ .

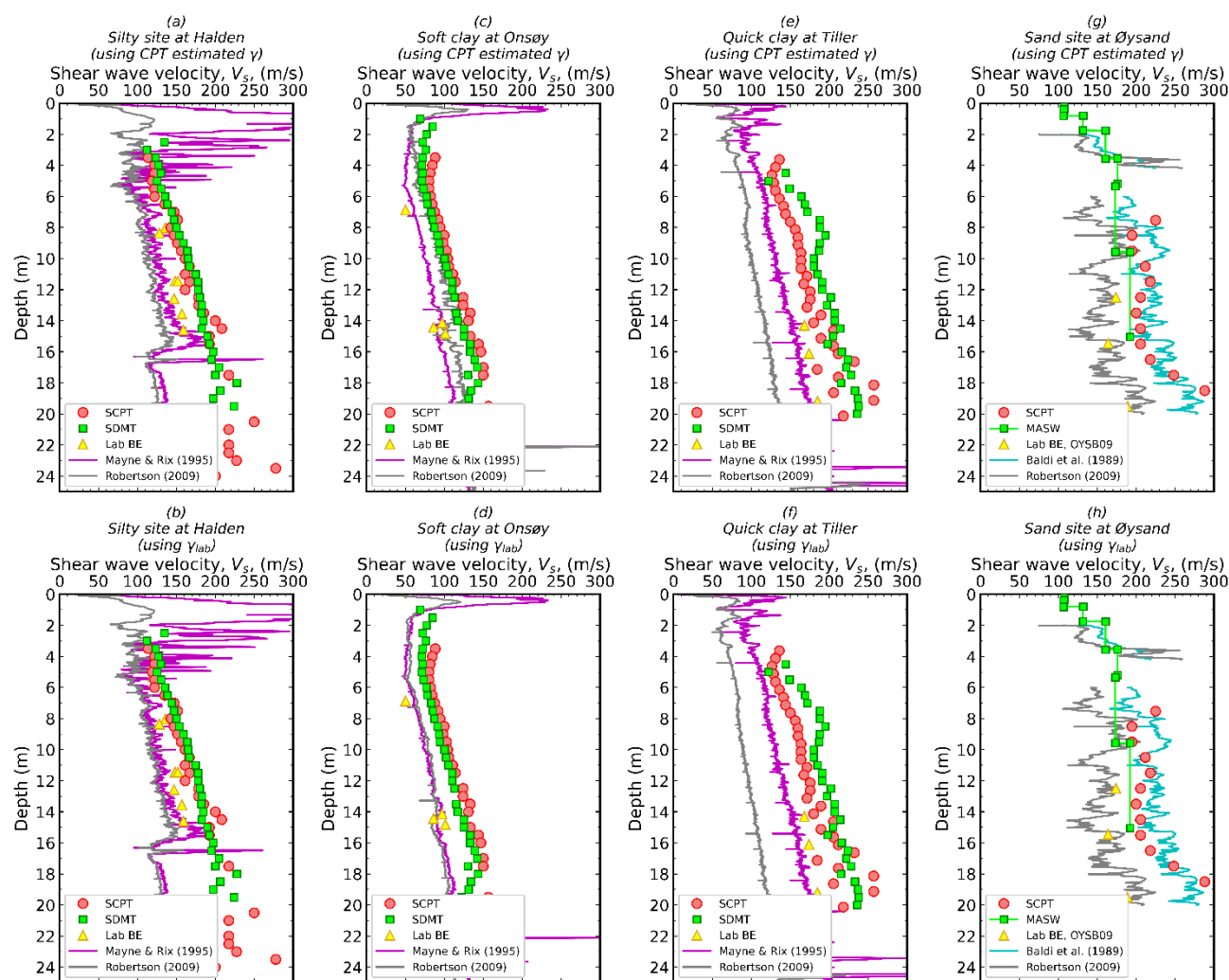


**Figure 4.6.**  $V_s$  measurements and estimations for: (a) Silty site at Halden using CPTU-based derived  $\gamma$ , (b) silty site at Halden using the best estimate  $\gamma$  from laboratory measurements, (c) soft clay at Onsøy using CPTU-based derived  $\gamma$ , (d) soft clay at Onsøy using the best estimate  $\gamma$  from laboratory measurement, (e) quick clay at Tiller using CPTU-based derived  $\gamma$ , (f) quick clay at Tiller using best estimate  $\gamma$  from laboratory measurements, (g) sand at Øysand using CPTU-based derived  $\gamma$ , and (h) sand at Øysand using best estimate  $\gamma$  from laboratory measurements.

#### 4.7. Small strain shear modulus, $G_0$

If  $\gamma$  and  $V_s$  are measured,  $G_0$  is derived from Elastic Theory (and sometimes it can be referred to

as measured  $G_0$ ). However, in engineering practice, the seismic tests are generally not included in the scope of work, so these measured parameters are estimated from correlations, which can produce erroneous results. In Figure 4.7, the results of measured  $G_0$  and CPTU-derived profiles for all four sites are presented. Laboratory Bender element results are used as a benchmark. It is observed that for Halden and Onsøy, the agreement appears to be very good when best estimate  $\gamma$  is used. It is seen that for Halden, in situ measured  $G_0$  and the profile estimated by CPTU-based correlation agrees very well with the results from bender elements tests. The agreement is also improved between SCPTU/SDMT measured  $G_0$  and the CPTU-based correlation for the Onsøy results when best estimate  $\gamma$  is used.  $G_0$  measurements and estimations for Øysand (plotted in Figure 4.7d) show that CPT derived estimations are significantly lower than the measured values.

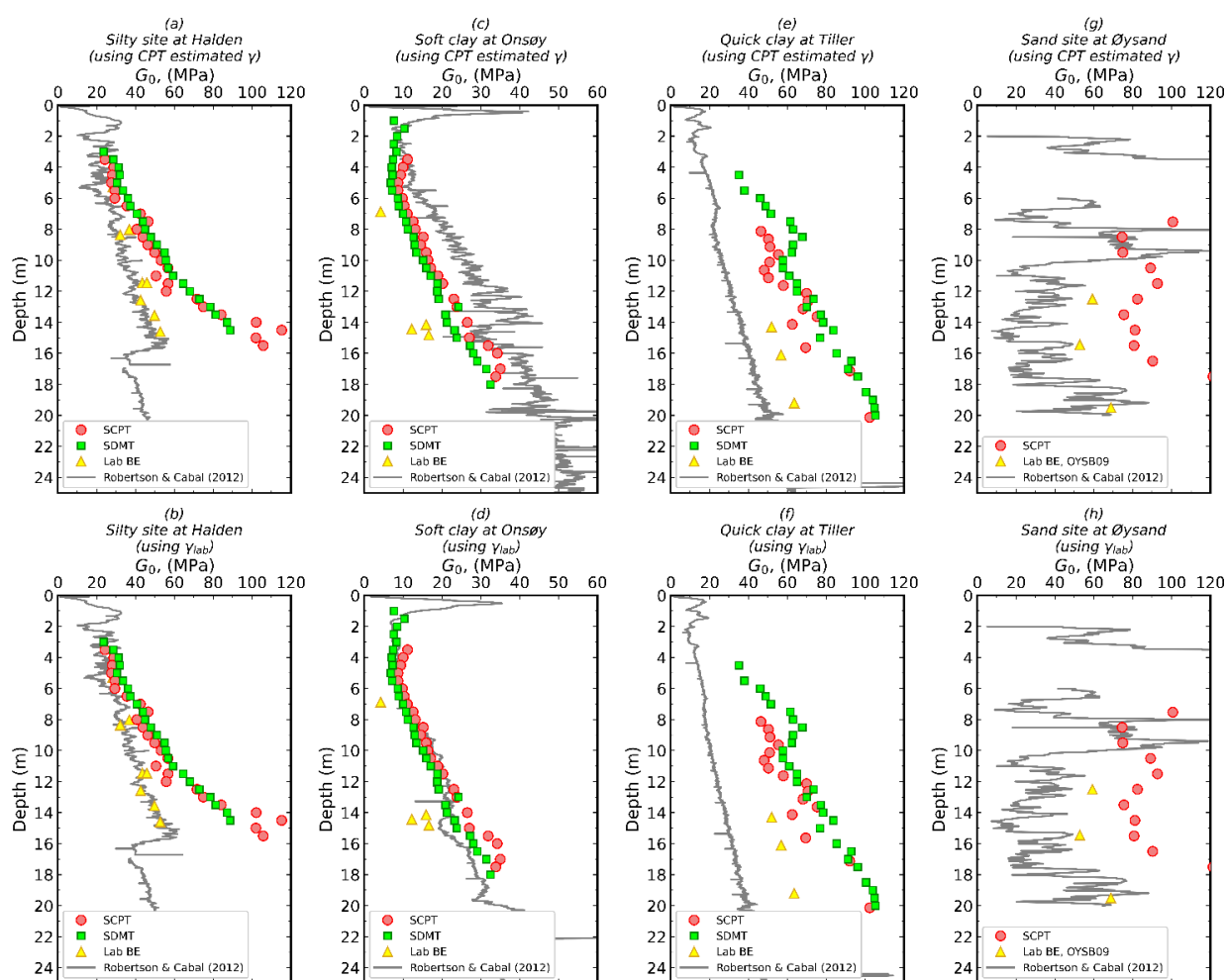


**Figure 4.7.**  $G_0$  profiles for: (a) Silty site at Halden using CPTU-based derived  $\gamma$ , (b) silty site at Halden using the best estimate  $\gamma$  from laboratory measurements, (c) soft clay at Onsøy using CPTU-based derived  $\gamma$ , (d) soft clay at Onsøy using the best estimate  $\gamma$  from laboratory measurements, (e) quick clay at Tiller using CPTU-based derived  $\gamma$ , (f) quick clay at Tiller using best estimate  $\gamma$  from laboratory measurements, (g) sand at Øysand using CPTU-based derived  $\gamma$ , and (h) sand at Øysand using best estimate  $\gamma$  from laboratory measurements.

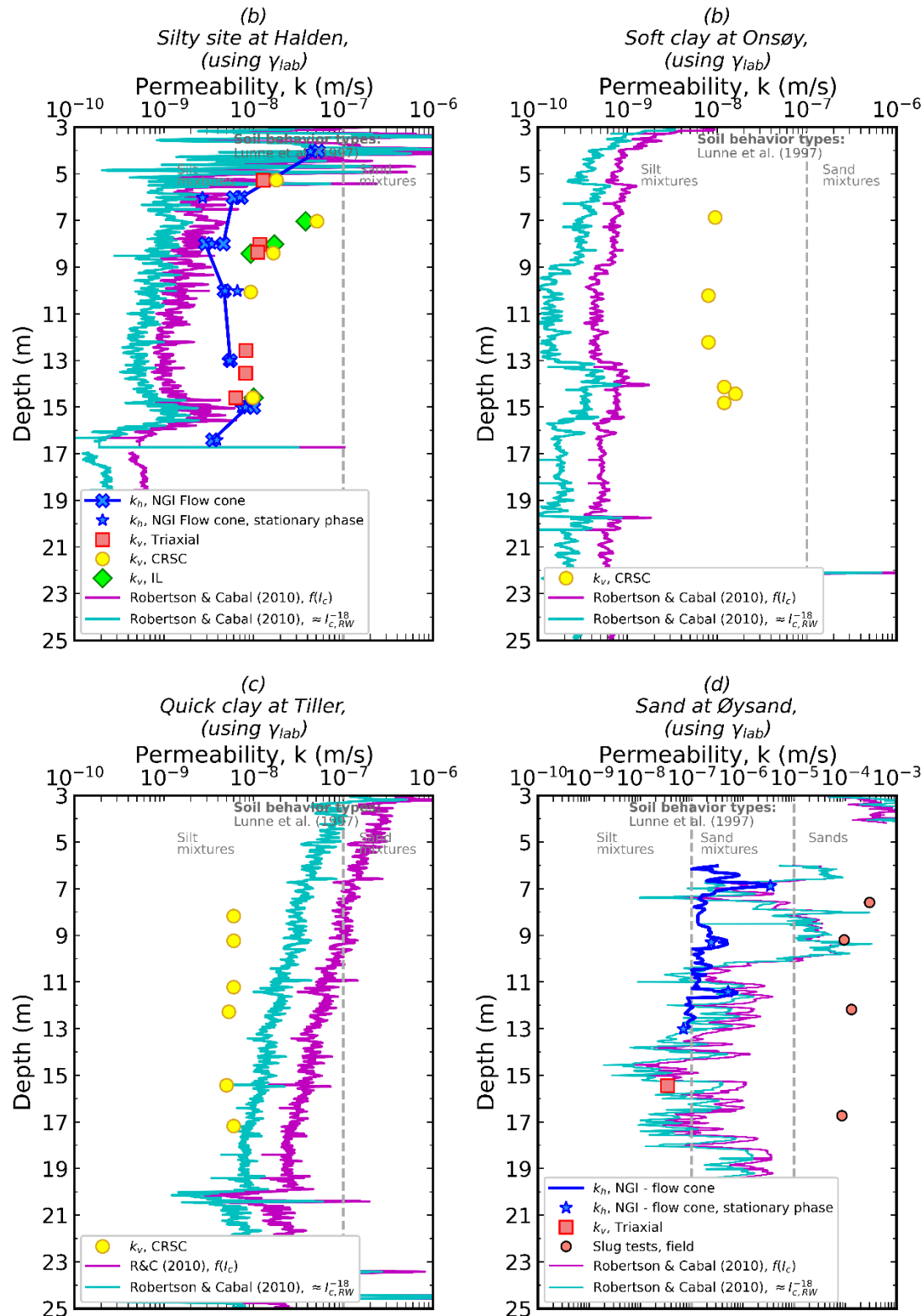


**Figure 4.8.** Measurements and estimations of  $k_h$  for: (a) Silty site at Halden, (b) soft clay at Onsøy, (c) quick clay at Tiller, (d) and sand at Øysand.

However, all in situ measured  $G_0$  overestimate in comparison with the laboratory Bender element results. As mentioned in Section 4.7 for  $V_s$ , the corrections linking cone parameters to  $G_0$

may be fortuitous. The researchers in [38] and [36] suggested that it was the horizontal stresses and stiffnesses that influence  $q_t$ , and that  $q_t$  correlates better with  $G_{hh}$ . This idea is further supported by the researchers in [37] who, using the same and additional data, suggested that  $V_{hh}$  correlates better to  $q_t$  than  $V_{vh}$  does [34].

#### 4.8. Permeability, $k_h$

It is often desirable to try and establish an idea of the ground's likely permeability. However, as expected, there is a wide discrepancy between the results, as measuring  $k_h$  remains a difficult task. It can be seen from Figure 4.8 that the permeability (expressed in m/s) is underestimated by an order of magnitude at Halden and Onsøy when using the derived unit weights, but about right or overestimating at Tiller. When the correct  $\gamma$  are used, the results get worse at Halden and Onsøy, and the previous agreement at Tiller is lost. These changes are a result of the influence of unit weight in the calculations of  $I_c$ , which is used in these equations.

Simply using the soil behaviour type of Table 3.2 would give wider bands of likely permeability but to 1 to 2 orders of magnitude. It is worth noting that at Halden, permeability values are available from laboratory oedometer tests and in situ flow cone tests ([39]). Moreover, an order of magnitude difference in these two test methods is observed, with the former being essentially vertical and the latter horizontal, and the CPTU derived values are closer to the flow cone tests. The results for the Øysand site are summarized in Figure 4.7 (d). The NGI flow cone results are believed to be the most trustworthy. Discrepancies are observed between measurement and CPTU estimations (based on [33]).

## 5. Discussion

The reliability of each correlation for each soil type and site is summarized in Table 5.1, where a summary of evaluation on a scale from A (very good) to D (very bad) is presented. With reference to Section 3, each correlation has been given a number, with the parameter that is needed noted alongside. The reliability is derived from the author's analysis and interpretation of the presented data. Most correlations use CPTU measured or derived parameters, and few use shear wave velocity,  $V_s$ , as measured by the seismic cone, SCPTU. Importantly, several correlations use  $\sigma'_{v0}$  or  $\sigma_{v0}$ , which needs  $\gamma$  as an input. This dependency on one correlation as input to another leads to more uncertainties, which are evaluated below in Table 5.1. For correlations using  $\gamma$  as an input, CPTU based  $\gamma$  profiles from [16] and [15] correlations are very similar. For simplicity, only the correlation in [16] was selected to be used when considering the reliability of derived parameters considered in Table 5.1 using derived or actual  $\gamma$  profiles as input.

Scale for reliability in Table 5.1: **A** very good, **B** reasonable, **C** not good, and **D** very bad. In the boxes where 2 letters are separated by a slash, the first letter shows the reliability scale for the results when the CPTU-based  $\gamma$  is used and the 2<sup>nd</sup> letter is used to rate the results when the best estimate  $\gamma$  from high quality laboratory tests is achieved.

Some general findings from Table 5.1 are listed below. It is worth mentioning that we agreed to use one single correlation to estimate  $\gamma$  from CPTU, which is that in [16]. This method is arbitrarily selected and does not show any preferences or relation to the ratings in Table 5.1.



**Table 5.1.** Summary of evaluations of reliability for all correlations and sites.

Site Parameter	Correlation No. in this paper and input parameter required	Soft clay at Onsøy	Silt at Halden	Quick clay at Tiller	Sand at Øysand	Comments
$\gamma$	1. SBT	B/C	B	B	B	Using figure d
	2. $R_f, q_t$	C	D	D	C	
	3. $f_s$	C	D	D	B	
	4a. $V_s$	C	C	B	B	
	4b. $V_s, \sigma'_{v0}$	B	C	B	C	
OCR	5a. $q_t, \sigma'_{v0}$	B/D	-	D/B	-	
	5b. $u_2$	B/D	-	D/C	-	
	6. $F_r, Q_t$	D/B	-	D/D	-	
$K_0$	7a. $q_t, \sigma'_{v0}$	B/C	D/B		-	
	7b. $q_t, \sigma'_{v0}$	B/D	D/B		-	
$s_u$	8. $F_r, N_{kt}$	D	B	A	-	
	9. $B_q V_s N_{kt}, \sigma_{v0}$	D	B	A	-	
	10. $B_q V_s N_{\Delta u}, \sigma_{v0}$	D	C	D	-	
$\phi$	11. $Q_{tn}$	-	-	-	B & A	
	12. $\phi_{cv}, Q_{tn,cs}$	-	-	-	C & B	
	13. $V_s, \sigma'_{v0}$	-	-	-	A & A	
$V_s$	14. $q_t, \sigma'_{v0}$	-	-	-	B/B	Only for sand
	15. $q_t$	C	D/D	D/D	-	
	16. $I_c, q_t, \sigma_{v0}$	A/C	D	D/D	C/C	
$G_0$	17. $I_c, q_t, \sigma_{v0}$	C/B	D/D	D/D	D/D	
$k_v$	18. $I_c$	D/D	D/D	D/D	D/D	

- For  $\gamma$ 
  - The SBT chart in [14], combined with tabulated values for each zone, as summarised by [13], appears to work best but can fail to show gradual changes due to the coarseness or suggested values. It is also affected by the assumed gamma used initially.
  - Correlations based on  $f_s$  or  $F_r$  and  $q_t$  do not work very well, while those based on  $V_s$  seem to work better for highly sensitive clay at Tiller and not good for silt at Halden, soft clay Onsøy, and sand at Øysand.
- For OCR
  - ⊖ Correlations can be checked only for Onsøy and Tiller clays due to the difficulty of interpreting the CRCS in sands and silts.
  - ⊖ For the soft clays at Onsøy, the correlations based on  $q_t$  and  $u_2$  seem initially to work well when the CPTU-based derived  $\gamma$  is used but poorly once the best estimate from laboratory measurements are used.
  - For the quick clay at Tiller, none of the correlations work initially but there is some improvement with equation 5 using the best estimate  $\gamma$  derived from high quality samples.

- Yield stress may be a better parameter to link correlations to in the future.
- For  $K_0$ 
  - correlations can be checked only for soft clay at Onsøy and silt at Halden, and the results appear promising for both.
  - For soft clay at Onsøy, agreement with pressuremeter data becomes worse when best estimate  $\gamma$  is used, showing initial agreement was rather fortuitous.
  - For silt at Halden, the reverse appears to be true.
- For  $s_u$ 
  - The  $N_{kt}$  correlation based on  $F_r$  does not work at any of the sites.
  - The  $N_{kt}$  and  $N_{\Delta u}$  correlations based on  $B_q$  work reasonably well for silt at Halden but does not work well for soft clay at Onsøy. Moreover, sensitive clay at Tiller seems to work very well.
- For  $\phi_p$  (evaluated only for the Øysand sand)
  - Correlations based on  $Q_{tn}$  or  $\phi_{cv}$ ,  $Q_{tn,cs}$  may provide a conservative estimate of  $\phi_p$ , and the assumption of  $\phi_{cv}$  has a high impact on any estimated values of  $\phi_p$ .
  - Correlations based on  $V_s$  are more reliable and show better agreement. Nonetheless, any error in deriving  $V_s$  will have significant implications in the estimation of  $\phi_p$ .
- For  $V_s$ 
  - For all the clay/silt sites, the reliability appears poor generally when using the CPTU-based derived  $\gamma$ , although there is some promise at Halden (silt) using correlation no. 14 and for Onsøy (soft clay) using correlation no. 16. However, these two agreements are shown to be fortuitous, as they both become worse once the best estimate  $\gamma$  from laboratory measurements are used.
  - For Øysand (sand), the influence of  $\gamma$  is minimal, and the correlation base on  $q_t$ ,  $\sigma'_{v0}$  provides the best fit with the field values of  $V_s$ .
- For  $G_0$ 
  - For the two clay sites at Onsøy and Tiller, the Halden silt and Øysand sand predictions are poor with little change when the best estimate  $\gamma$  from laboratory measurements is used.
- For  $k$ 
  - Predictions in all cases are relatively poor.
  - The best -recommended- way to gain information on soil permeability from a CPTU test is to run a dissipation test. By stopping the cone penetration at a pre assigned depth and letting the pore water pressure around the cone dissipate until it reaches the equilibrium pressure (or until it reached a required degree of pore pressure dissipation – generally greater than 50% of dissipation), the acquired data can be used to estimate the coefficient of consolidation in the horizontal direction,  $c_h$  which can be converted into permeability if the nature of clay is known (see [40]).

Furthermore, some overall observations are listed below:

- Two correlations that are based on  $f_s$  and/ or  $F_r$  (No. 3 and 8) both give very bad predictions.
- In most cases, when using the best estimate  $\gamma$  input from laboratory measurements, a better fit is obtained with the benchmark results from laboratory tests on high quality samples (or high quality SBP for  $K_0$  comparisons). However, in some cases, the fit gets worse once  $\gamma$  is

changed from CPTU-based derived profiles to best estimate profiles from laboratory measurements, and in a few cases, it makes neglectable improvements.

- Correlations No. 9 and 10, where  $N_{kt}$  and  $N_{\Delta u}$  are functions of  $B_q$ , work well for the silts at Halden and quick clay at Tiller and reasonably well for the soft clay at Onsøy.
- One limitation of the investigation presented herein and of the rating of correlations as included in Table 5.1 is the range of soil types investigated, which do not include overconsolidated clays ( $OCR > 2$ ), very dense sand, and several other soils. However, from other papers, results between several correlations were used to derive various soil parameters in overconsolidated clays at Cowden. For example, it is seen that these correlations used without care (with erroneous  $\gamma$  and ground water level as input and global coefficients), significantly overestimate  $V_s$ ,  $G_0$  and constrained modulus,  $M$  (see for instance [34, 41]).
- Although many of the correlations do not give highly reliable results that fully match the benchmarks from laboratory tests resulting in high quality samples, the trend with depth is realistic. Variation with depth is, in most cases, very similar to the benchmark profiles, although the absolute values can be quite different.
- Finally, site specific constants (or coefficients) should be established beforehand based on laboratory tests, resulting on high quality samples. If these results become available at a later stage of the project, it is important to use previous experience and knowledge for the soil types where CPTU-based correlations will be applied. In the case of  $OCR$ ,  $K_0$ , and  $s_u$  correlations used herein, the best fit is achieved when the coefficients involved in correlations no. 5a, b, 7a, b, 8, 9, and 10 are back calculated for each layer than one value for the entire profile. We changed the constants in correlation no. 5a, b from 0.33 to 0.5 (for the correlation no. 5a utilising  $q_t$ ) and from 0.54 to 0.3 (for the correlation no. 5b utilising  $u_2$ ) for Onsøy to obtain a more satisfactory match with laboratory  $OCR$  profiles. The same procedure is carried out for  $K_0$ , with changing the constants in correlation no. 7a from 0.1 and using this as a global number for the entire soil profile to 0.2 for the first 10.5 m and 0.15 for the rest of the soil profile. Even though these changes might seem very minor, the impact on the results can be as high as 30%. Again, using Onsøy data, a back calculation exercise is performed for the  $N_{kt}$  for the layer from 11 m to 14 m, showing that the best estimate  $N_{kt}$  can be as low as 8. Although  $N_{kt}$  is varied for each layer, even within the same layer, sublayers of soils can be present, requiring adjustments of these factors to better reflect their state in situ.

## 6. Recommendations

The main recommendation is that, whenever possible, local correlations should be established and used; for large and important projects, this is a must. The importance of linking CPTU parameters with results from high quality laboratory tests cannot be overstressed if efficiency in design is to be achieved. Always revisit processing of data when site specific information becomes available, and site-specific correlations are established. They are far from foolproof. Soil properties should be treated with caution if they are derived without basic input information.

In some cases, simple laboratory tests to determine  $\gamma$  or water content are available, although no advanced laboratory tests have been carried out. In such cases, it is recommended to use the site specific  $\gamma$  data and not the  $\gamma$  from CPTU or  $V_s$  correlations.

Since many of the correlations need  $\gamma$  as an input, it will be very useful if new and better correlations of  $\gamma$  could be established. It is suggested that the following should be considered: Grouping of soils, using CPTU parameters and  $V_s$  from seismic cone tests when possible, and using machine learning techniques. Another option might be the utilization of dielectric CPTU where in-place measurements of water content could add in the estimation of unit weights.

If contractors use software with correlations for evaluating and reporting soil parameters, it is important that they state the uncertainties involved with the derived parameters, and these parameters should be used only for preliminary foundation design. Likewise, it is important that consultants receiving the reports use the correlated parameters with care.

Furthermore, checking correlations, as presented in this paper, should be extended to other soil types and especially to overconsolidated clays with  $OCR > 2$ .

## 7. Summary and conclusions

Commercial software packages that utilise published CPTU correlations are frequently used for quick presentation of soil parameters such as soil unit weight, over consolidation ratio, lateral stress ratio, undrained shear strength, and shear wave velocity. It is a well-known fact that such correlations are not globally valid, but many practitioners use the parameters obtained this way even in foundation design.

At the Norwegian soft clay, quick clay, silt, and sand national geo test sites (NGTS), high quality sampling and laboratory testing have resulted in consistent representative and reliable benchmark soil parameters. Unique for this study is that the ground freezing technique was used for sampling undisturbed sand followed by high quality laboratory tests. High quality CPTU and shear wave velocities data are also available at the sites in addition to a new “flow cone penetrometer” for measuring in situ permeability.

Using these high-quality soil parameters as benchmarks for each parameter calculated in this paper has given an excellent and novel opportunity to evaluate the validity of the soil parameters derived from published CPTU correlations used in commercial software packages.

Since several of the correlations rely on input on soil unit weight, this parameter is very important. The systematic comparison of  $\gamma$  from laboratory tests with values obtained from various correlations shows that this can give very large differences, especially for the 2 clays and silt sites included in the study. When these correlation-derived  $\gamma$  values are used as input for CPTU correlations to other soil parameters such as OCR,  $K_0$ , and  $s_{uC}$ , large differences relative to the benchmark values are found in most cases. When using  $\gamma$  measured from laboratory tests, large improvements in closeness to benchmark values can be observed in most cases. In very few cases, the use of laboratory determined  $\gamma$  does not make improvements. However, an important recommendation from this is that if laboratory values of  $\gamma$  should be available (although no advanced laboratory tests have been performed), this should be used than CPTU-based derived  $\gamma$ . It is also recommended to try and improve the CPTU-based derived  $\gamma$  by better grouping soils, using combined CPTU measurements and  $V_s$  measurements from seismic cones etc. This is particularly important with the urge of using machine learning, where a “bad” profile of soil unit weight with depth tends only to poorly affect the other parameters values, as determined from CPTU.

A few correlations use inputs from  $f_s$  (for  $\gamma$ ) or  $R_f$  (for  $s_u$ ) and these give bad results; thus, it is recommended not to use them.

Finally, this study shows the need to use site specific correlations whenever possible.

### Author contributions

Tom Lunne: Conceptualization, Formal analysis, Investigation, Methodology, Project administration, Resources, Validation, Writing – original draft, Writing – review & editing; Luisa Dhimitri: Conceptualization, Data curation, Formal analysis, Validation, Visualization, Writing – original draft, Writing – review & editing; John Powell: Conceptualization, Data curation, Formal analysis, Validation, Visualization, Writing – original draft, Writing – review & editing; Santiago Quinteros: Data curation, Validation, Visualization, Writing – original draft, Writing – review & editing.

### Acknowledgements

The authors would like to acknowledge the guidance from NGI colleague Marit Støvne who has several times helped us with spelling mistakes and format issues (not for the first time).

### Use of AI tools declaration

The authors declare they have not used Artificial Intelligence (AI) tools in the creation of this article.

### Conflict of interest

All authors declare no conflicts of interest in this paper.

### References

1. L'Heureux J-S, Lunne T (2019) Characterization and Engineering properties of Natural Soils used for Geotesting. *AIMS Geosci* 6: 35–53. <https://doi.org/10.3934/geosci.2020004>
2. L'Heureux JS, Lunne T, Lacasse S, et al. (2017) Norway's National GeoTest Site Research Infrastructure (NGTS), *Proceedings of the 19th International Conference on Soil Mechanics and Geotechnical Engineering*, Seoul.
3. Gundersen AS, Hansen RC, Lunne T, et al. (2019) Characterization and engineering properties of the NGTS Onsøy soft clay site. *AIMS Geosci* 5: 665–703. <https://doi.org/10.3934/geosci.2019.3.665>
4. L'Heureux JS, Lindgård A, Emdal A (2019) The Tiller-Flotten research site: Geotechnical characterization of a very sensitive clay deposit. *AIMS Geosci* 5: 831–867. <https://doi.org/10.3934/geosci.2019.4.831>
5. Blaker Ø, Carroll R, Paniagua P, et al. (2019) Halden research site: geotechnical characterization of a post glacial silt. *AIMS Geosci* 5: 184–234. <https://doi.org/10.3934/geosci.2019.2.184>

6. Quinteros S, Gundersen A, L'Heureux JS, et al. (2019) Øysand research site: Geotechnical characterisation of deltaic sandy-silty soils. *AIMS Geosci* 5: 750–783. <https://doi.org/10.3934/geosci.2019.4.750>
7. Long M, Lunne T, Forsberg CF (2003) Characterisation and engineering properties of Onsøy clay, In: Tan TS, Phoon KK, Hight DW, et al. Eds., *Characterisation and engineering properties of natural soils*, Singapore, Balkema, 395–427.
8. ISO 22476-1, Geotechnical investigation and testing—Field testing—Part 1: Electrical cone and piezocone penetration test, Standards from ISO are available both individually, directly through the ANSI webstore, and as part of a Standards Subscription.
9. Lunne T, Strandvik S, Kåsin K, et al. (2018) Effect of cone penetrometer type on CPTU results at a soft clay site in Norway, *Cone Penetration Testing 2018*, Delft, The Netherlands, Taylor & Francis, 417–422.
10. Paniagua P, Lunne T, Gundersen A, et al. (2021) CPTU results at a silt test site in Norway: Effect of cone penetrometer type, *IOP Conference Series: Earth and Environmental Science*, IOP Publishing Ltd.
11. Lindgård A, Gundersen A, Lunne T, et al. (2018) Effect of cone type on measured CPTU results from Tiller-Flotten quick clay site. *Proceedings Geoteknikkdagen 2018 Oslo*, 38: 1–15.
12. Quinteros VS (2022) *On the initial fabric and triaxial behaviour of an undisturbed and reconstituted fluvial sand*, Imperial College London.
13. Lunne T, Powell JJM, Robertson PK (1997) *Cone Penetration Testing in Geotechnical Practice*, New York. CRC Press. <https://doi.org/10.1201/9781482295047>
14. Robertson PK, Campanella RG, Gillespie D, et al. (1986) Use of Piezometer Cone Data, *Use of In-Situ Tests in Geotechnical Engineering, In-Situ 86, (GSP 6)*, 1263–1280. Available from: [https://www.researchgate.net/publication/285689813\\_Use\\_of\\_Piezometer\\_Cone\\_Data](https://www.researchgate.net/publication/285689813_Use_of_Piezometer_Cone_Data).
15. Robertson PK, Cabal KL (2010) Estimating soil unit weight from CPT, *2nd International Symposium on Cone Penetration Testing, CPT 10*, California, USA, 447–454.
16. Mayne PW, Peuchen J (2013) Unit weight trends with cone resistance in soft to firm clays, *Geotechnical and Geophysical Site Characterization: Proceedings of the 4th International Conference on Site Characterization ISC-4*, Boca Raton, 1: 903–910.
17. Mayne PW (2014) Interpretation of geotechnical parameters from seismic piezocone tests, In: Robertson PK, Cabal KI, Eds., *3rd International Symposium on Cone Penetration Testing*, Las Vegas, Nevada, USA, ISSMGE Technical Committee TC, 102: 47–73.
18. Mayne PW (2007) *NCHRP Synthesis: Cone Penetration Testing State-of-Practice*, Transportation Research Board, National Academy Press, Washington, DC, 118. Available from: [www.trb.org](http://www.trb.org).
19. Mayne PW (2001) Stress-strain-strength-flow parameters from enhanced in-situ tests, *On In Situ Measurement of Soil Properties and Case Histories*, Bali, Indonesia, 27–48.
20. Mayne PW (2005) Keynote: integrated Ground Behavior: In Situ and Lab Tests, In: Di Benedetto H, Doanh T, Geoffroy H, et al. Eds., *Deformation Characteristics of Geomaterials*, Lyon, 154–176.
21. Been K, Quiñonez A, Sancio RB (2010) Interpretation of the CPT in engineering practice, In: Robertson PK, Mayne PW, Eds., *2nd International Symposium on Cone Penetration Testing*, Huntington Beach, CA, USA, 1–18.

22. Robertson PK, Cabal KL (2010) *Guide to Cone Penetration Testing for Geotechnical Engineering*, Signal Hill, California, Gregg Drilling & Testing Inc.
23. Ladd CC, Foott R (1974) New design procedure for stability of soft clays. *J Geotech Eng Div* 100: 763–786. <https://doi.org/10.1061/AJGEB6.0000066>
24. Kulhawy FH, Mayne PW (1990) *Manual on estimating soil properties for foundation design*, United States.
25. Tavenas F, Leroueil S (1987) State-of-the art, laboratory and in situ stress strain-time, *International Symposium on Geotechnical Engineering of Soft Soils*, 1–146.
26. Mayne PW, Peuchen J (2022) Undrained shear strength of clays from piezocone tests: A database approach, In: Gottardi G, Tonni L, Eds., *Cone Penetration Testing 2022*, Bologna, CRC Press, 546–551.
27. Mayne PW, Ethan C, James G (2023) The cone penetration test: A CPT Design Parameter Manual. Available from: ConeTec Group, Canada.
28. Jefferies M, Been K (2015) *Soil liquefaction: a critical state approach*, CRC Press.
29. Uzielli M, Mayne P, Cassidy M (2013) Probabilistic assignment of design strength for sands from in-situ testing data, *Advances in Soil Mechanics & Geotechnical Engineering (series)*, Amsterdam, IOS-Millpress, 214–227. <https://doi.org/10.3233/978-1-61499-163-2-214>
30. Baldi G, Bellotti R, Ghionna V, et al. (1986) Interpretation of CPTs and CPTUs; 2nd part: drained penetration of sands, *Proceedings of the Fourth International Geotechnical Seminar*, Singapore, 143–156.
31. Mayne PW, Rix GJ (1995) Correlations between shear wave velocity and cone resistance in natural clays. *Soils Found* 35: 107–110. [https://doi.org/10.3208/sandf1972.35.2\\_107](https://doi.org/10.3208/sandf1972.35.2_107)
32. Robertson PK (2009) Interpretation of cone penetration tests—A unified approach. *Can Geotech J* 46: 1337–1355. <https://doi.org/10.1139/T09-065>
33. Robertson PK (2010) Estimating in-situ soil permeability from CPT & CPTu, *2nd International Symposium on Cone Penetration Testing*, California, USA. 2: 535–542.
34. Powell JJM, Dhimitri L (2022) Watch out for the use of global correlations and “black box” interpretation of CPTU data, *Cone Penetration Testing 2022*, Bologna, CRC Press/Balkema, 651–656.
35. Quinteros VS, Carraro JAH, L’Heureux J-S, et al. (2024) Disturbance of sand samples obtained by piston samplers and ground freezing, *Proceedings of the 8<sup>th</sup> international Symposium on Deformation Characteristics of Geomaterial (IS-Porto 2023)*. 544. <https://doi.org/10.1051/e3sconf/202454403001>
36. Powell JJM, Dhimitri L, Ward D, et al. (2016) Small Strain Stiffness assessments from in situ tests—revisited, *Geotechnical and Geophysical Site Characterisation 5*, Sydney, Australia, Australian Geomechanics Society, 1253–1258.
37. Long M (2022) Practical use of shear wave velocity measurements from SCPTU in clays, *Cone Penetration Testing 2022*, CRC Press/Balkema, 28–52.
38. Powell JJM, Butcher AP (2004) Small Strain Stiffness assessments from in situ tests, *ISC2 Porto*, Porto, 1717–1722.
39. Gundersen AS, Carotenuto P, Lunne T, et al. (2019) Field verification tests of the newly developed flow cone tool—In-situ measurements of hydraulic soil properties. *AIMS Geosci* 5: 784–803. <https://doi.org/10.3934/geosci.2019.4.784>



40. Jamiolkowski M, Ladd CC, Germaine JT, et al. (1985) New developments in field and laboratory testing of soils, *11th International Conference on Soil Mechanics and Foundation Engineering*, San Francisco, California, 57–153.
41. Dhimitri L, Powell JJM, (2023) Constrained modulus of fine-grained soils from in situ based correlations and comparison with laboratory tests, *Proceedings of the 8<sup>th</sup> international Symposium on Deformation Characteristics of Geomaterial*. Available from: <https://www.issmge.org/uploads/publications/121/122/isdcg2023-165-1-c.pdf>.



AIMS Press

© 2025 the Author(s), licensee AIMS Press. This is an open access article distributed under the terms of the Creative Commons Attribution License (<https://creativecommons.org/licenses/by/4.0>)